Molecular Characterisation of Transport Mechanisms at the Developing Mouse Blood–CSF Interface: A Transcriptome Approach

Shane A. Liddelow[1]*, Sally Temple[2,3], Kjeld Møllgård[5], Renate Gehwolf[4], Andrea Wagner[4], Hannelore Bauer[4], Hans-Christian Bauer[4], Timothy N. Phoenix[2,6], Katarzyna M. Dziegielewska[1], Norman R. Saunders[1]

1 Department of Pharmacology, The University of Melbourne, Melbourne, Victoria, Australia, 2 Neural Stem Cell Institute, Regenerative Research Foundation, Rensselaer, New York, United States of America, 3 University at Albany, Albany, New York, United States of America, 4 Department of Organismic Biology, University of Salzburg, Salzburg, Austria, 5 Institute of Cellular and Molecular Medicine, University of Copenhagen, Copenhagen, Denmark, 6 Department of Developmental Neurobiology, St. Jude Children's Research Hospital, Memphis, Tennessee, United States of America

Abstract

Exchange mechanisms across the blood–cerebrospinal fluid (CSF) barrier in the choroid plexuses within the cerebral ventricles control access of molecules to the central nervous system, especially in early development when the brain is poorly vascularised. However, little is known about their molecular or developmental characteristics. We examined the transcriptome of lateral ventricular choroid plexus in embryonic day 15 (E15) and adult mice. Numerous genes identified in the adult were expressed at similar levels at E15, indicating substantial plexus maturity early in development. Some genes coding for key functions (intercellular/tight junctions, influx/efflux transporters) changed expression during development and their expression patterns are discussed in the context of available physiological/permeability results in the developing brain. Three genes: *Secreted protein acidic and rich in cysteine* (*Sparc*), *Glycophorin A* (*Gypa*) and *C* (*Gypc*), were identified as those whose gene products are candidates to target plasma proteins to choroid plexus cells. These were investigated using quantitative- and single-cell-PCR on plexus epithelial cells that were albumin- or total plasma protein-immunopositive. Results showed a significant degree of concordance between plasma protein/albumin immunoreactivity and expression of the putative transporters. Immunohistochemistry identified SPARC and GYPA in choroid plexus epithelial cells in the embryo with a subcellular distribution that was consistent with transport of albumin from blood to cerebrospinal fluid. In adult plexus this pattern of immunostaining was absent. We propose a model of the cellular mechanism in which SPARC and GYPA, together with identified vesicle-associated membrane proteins (VAMPs) may act as receptors/transporters in developmentally regulated transfer of plasma proteins at the blood–CSF interface.

Introduction

The central nervous system functions in a well-controlled environment and is protected by a set of mechanisms known collectively as the blood–brain barrier [1]. These mechanisms are present at five distinct interfaces: (i) the blood–brain barrier proper at the level of the endothelium of the cerebral blood vessels; (ii) the arachnoid barrier between the cerebrospinal fluid (CSF) in the subarachnoid space and the dura; (iii) the pia/glia limitans between the CSF in the subarachnoid space and extracellular fluid of the brain, which is much more complex in the embryo; (iv) the CSF-brain barrier, which is only a significant barrier in the embryo, created by separation of the ventricular system from the extracellular fluid of the brain by strap junctions in the neuroependyma and (v) the blood–CSF barrier at the level of

the choroid plexus epithelial cells (**Fig. 1**). The importance of these barriers in normal neural development and in pathological conditions has been documented [2–5]. These same barrier mechanisms protect the brain from the effects of toxins and prevent the entry of many drugs [5,6].

Most studies of brain barrier properties have concentrated on the cerebral endothelial cell interface (blood–brain barrier) with much less work having been done on the choroid plexus interface [7]. In the developing brain the differentiation and growth of the choroid plexuses occurs much earlier than most of the vascularisation of the brain. Thus it has been suggested that in early development the main portal of entry from blood into brain is via the choroid plexuses and CSF rather than via the sparsely distributed cerebral blood vessels [1,8].
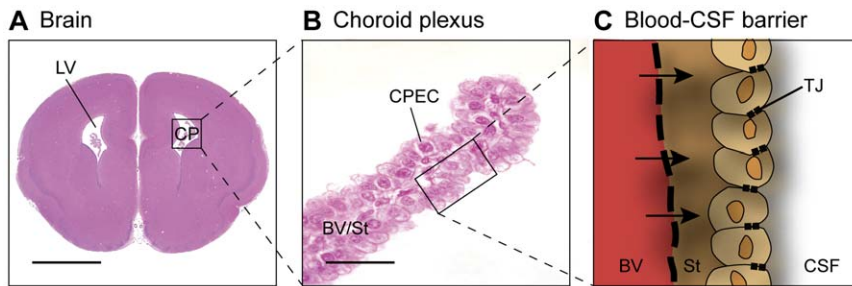
Figure 1. The choroid plexus and the blood–CSF barrier. A. The choroid plexuses are highly vascularised epithelial tissue that originates from the neuroependyma in the developing brain (ependyma in adult) and float freely in each of the brain ventricles (the two lateral, third and fourth). These specialised organs have two major functions: (i) to act as a diffusion barrier between the blood and the CSF; and (ii) they produce and secrete the CSF that fills the ventricles and subarachnoid spaces. **B.** The choroid plexuses are comprised of a central stroma with many blood vessels covered by a single layer of specialised epithelial cells, which rest on a thick basement membrane. **C.** The choroid plexuses are one of the circumventricular organs (i.e. they are positioned at sites around the margin of the ventricular system of the brain) and, like blood vessels in this region of the brain, the vessels of the choroid plexus stroma are fenestrated and the junctional strands linking adjacent endothelial cells are discontinuous. Accordingly, molecules are able to leave the blood vessels and enter the basement membrane of the plexus (arrows). However, a protective barrier is present in the choroid plexus, itself provided by tight, adherens, gap and other junctions between intimately apposed plexus epithelial cells – forming the blood–CSF barrier. The presence of many junctions between adjacent plexus epithelial cells from its first appearance in development means that the paracellular route for small molecules between blood and CSF is closed off in the embryo as well as in the adult. Abbreviations: BV, blood vessel; CP, choroid plexus; CPEC, choroid plexus epithelial cell; CSF, cerebrospinal fluid; LV, lateral ventricle; St, stroma; TJ, tight junction; Scale bar: 500 µm in A, 25 µm in B.
doi:10.1371/journal.pone.0033554.g001

The main characteristics of each brain barrier interface include a morphological component in addition to cellular transport mechanisms. The key morphological feature is the tight junctions between the cells of the interfaces: cerebral endothelial cells at the blood–brain barrier and epithelial cells at the choroid plexus blood–CSF barrier [1,9]. The cellular transport mechanisms encompass influx mechanisms for nutrients such as amino acids and vitamins, and efflux mechanisms, which are important barrier mechanisms that prevent the entry of many drugs and toxins into the brain [5,10]. In addition, there are ion exchange mechanisms and water channels that define the key features of the brain's internal environment which are essential for normal neuronal function [8].

A key question for understanding brain development lies in determining to what extent these barrier mechanisms are functional in the embryonic and fetal brain and whether there are barrier mechanisms that are specific to the developing brain. In spite of numerous claims over nearly 100 years based on belief and poor experimentation that embryonic brain barriers are 'immature', it is now clear that fundamental barrier properties are present very early in development (see [1,9]). Daneman and colleagues [2] have provided evidence of expression of numerous blood–brain barrier genes in the developing brain, but there is no equivalent information for the choroid plexuses.

An intriguing feature of CSF in the developing brain is its high concentration of protein—which has been identified in all mammalian species studied so far [11–15]. Experimental evidence showed that most of these proteins in CSF originate from blood plasma [15–18] although synthesis in situ in the choroid plexus also contributes [19]. Previous studies suggest that a specific recognition mechanism for individual proteins is present at the blood–CSF barrier, especially during early stages of brain development [16–18,20,21] but the molecular identity of this mechanism remains elusive. One molecule, secreted protein acidic and rich in cysteine (SPARC), has been proposed to be involved in targeting albumin to the blood-CSF interface—although it seems likely that SPARC is not the only transporter involved [22].

In this study we have used Affymetrix GeneChip arrays to describe the transcriptome of embryonic and adult mouse lateral ventricular choroid plexus and mined these datasets for intercellular junction and specific transporter genes. It is the first to describe the lateral ventricular choroid plexus transcriptome in the mouse embryo (at embryonic day 15) and to identify a set of genes whose expression is enriched compared with the adult. A transcriptome analysis of adult mouse choroid plexus has been published previously [23]. We report that several genes coding for proteins known to be albumin-targeting in other systems, are expressed within a subset of epithelial cells of the choroid plexus that are also immunopositive for albumin. We propose a way by which this mechanism for protein transfer across choroid plexus epithelial cells could operate.

Materials and Methods

Ethics statement

All animal experiments were conducted in accordance with the Public Health Safety Policy on the Humane Care and Use of Laboratory Animals (National Institutes of Health). All animal research protocols were reviewed and approved by the State University of New York – University at Albany Institutional Animal Care and Use Committee and registered with the US Office of Laboratory Animal Welfare (International Animal Care and Use Committee Registration A3621-01).

Animal husbandry

Timed-pregnant and non-pregnant Swiss Webster female mice supplied by Taconic Farms Inc. (NY, USA) were used in this study. For general morphology and immunohistochemistry a range of embryonic (E) and postnatal (P) ages were used: E12, E13, E14, E15, E16, E19, P2, P15 and adult (10 weeks, 15–30 g). All embryos were staged according to the guidelines of Theiler [24]. For general histology paraffin-embedded brain sections from all ages were used ($n = 6$ animals at each age). For Affymetrix GeneChip arrays and qPCR validation lateral ventricular choroid plexuses from E15 ($n = 100$) and adult ($n = 30$) were used. For single-cell qPCR paraffin-embedded lateral ventricular choroid plexus sections from E15 and adult were investigated ($n = 6$ at each age). These ages were chosen as they correlate to the time when

there is the maximum (E15) and minimum (adult) percentage of plasma protein-positive epithelial cells in the choroid plexus (see below and **Table S1**).

Collection of brains for morphological studies

Embryonic animals were killed by decapitation, brains dissected out under cold 4% PHEM fixative (1.23 M paraformaldehyde, 1.29 M PIPES, 0.55 M HEPES, 0.20 mM EGTA, 0.16 M MgSO$_4$) and post-fixed by immersion in Bouin's solution (Sigma, St Louis, MO, USA) for 24 hours. Postnatal animals were killed by cervical dislocation and fixed by perfusion with cold 4% PHEM fixative, for 10 minutes at 70% of cardiac output. Following perfusion, brains were dissected out and post-fixed by immersion in Bouin's solution for 24 hours. Once fixed, all brains were washed in 70% ethanol until clear, embedded in paraffin wax (Sigma) and 5 µm coronal sections cut.

Collection of lateral ventricular choroid plexus

Animals were killed as above and brains dissected out under cold RNase-free phosphate buffered saline (PBS, pH 7.3). Cerebral hemispheres were separated and both lateral ventricular choroid plexuses removed and placed in fresh ice-cold RNase-free PBS. Plexuses were pooled from several litters, spun down, excess PBS removed, snap-frozen in liquid nitrogen and stored at −80°C. The choroid plexus consists of epithelium as well as blood vessels and mesenchymal stroma. However, the epithelium is the predominant cell type, suggested to represent up to 90% of the plexus tissue [25]. In this study lateral ventricular choroid plexus was taken *in toto*.

Microarray screen of lateral ventricular choroid plexus

Total RNA was extracted from pools of E15 and adult lateral ventricular choroid plexus (from a minimum of 10 individuals in each pool) using the RNeasy Mini Kit, Qiashredder columns and gDNA removal columns according to standard supplier protocol (Qiagen, Valencia, CA, USA). Approximately 2 µg of total RNA from each of the six independent samples (three E15, three adult) were processed and hybridised to a GeneChip Mouse Exon 1.0 ST Array (Affymetrix, Santa Clara, CA, USA) using standard procedures (www.affymetrix.com). Microarray hybridisation and gel capture was performed by the Microarray Core Facility at the University at Albany Centre for Functional Genomics (Rensselaer, NY, USA). Array experiments were conducted according to the Minimum Information About a Microarray Experiment (MIAME) guidelines [26]. A checklist of these guidelines is provided in **Table S2**. An excel spreadsheet of the full comparison dataset is provided as **Table S3** and the array data have been deposited into the Gene Expression Omnibus (GEO, http://www.ncbi.nlm.nih.gov/geo/) with series accession number (GSE33009) and sample accession numbers (GSM818292, GSM 818293, GSM818294, GSM818295, GSM818926, GSM818927).

Affymetrix data analysis. For gene level analysis, the Affymetrix Power Tools software (Affymetrix) was used to normalise scanned images and to summarise the probe set. Briefly, raw array data was RMA normalised (robust multichip analysis, [27]) per chip median and filtered to include the top 80th percentile of genes expressed. Following an un-paired *t*-test ($p<0.05$), a Benjamini-Hochberg false discovery rate correction [28,29] was applied before subjecting the list to a fold change cut-off of two. Further, more stringent discrimination of target lists was achieved using GoMiner^{TM} software (Application Build 253; [30]). Targets were sorted using a combination of molecular and biological gene ontology terms.

Real-Time qPCR validation

Total RNA was prepared from lateral ventricular choroid plexus as outlined above. First-strand cDNA was synthesised using a High Capacity RNA-cDNA conversion kit (Applied Biosystems, Carlsbad, CA, USA). Real-time PCR was performed using SYBR Green assay using the 7900HT Fast Real Time PCR System running SDS2.3 software (Applied Biosystems). Gene expression was determined relative to levels of expression of the transferrin receptor using the ΔΔCt method. Gene expression for transferrin receptor has been shown not to change during plexus development [31]. Standard deviations were calculated from triplicates of three separate samples in each instance. Primers for target genes were designed using the OligoPerfect^{TM} Designer (Invitrogen, Carlsbad, CA, USA) and are listed in **Table 1**.

Laser capture and single cell PCR

Laser-capture microdissection was performed on paraffin-embedded tissue sections of E15 and adult mouse lateral ventricular choroid plexus. Randomly selected sections containing lateral ventricular choroid plexus were immunostained with antibodies to mouse albumin raised in goat (1:5000, abcam, Cambridge, MA, USA, ab19194) or to mouse total plasma protein raised in rabbit (1:5000, DAKO, Glostrup, Denmark, ZO177). For a list and specification of antibodies refer to **Table 2**. After washing with PBS+Tween20, sections were incubated with appropriate secondary antibodies conjugated to peroxidase (donkey anti-goat, 1:1000, Millipore/Chemicon, Vienna, Austria, AP180P; goat anti-rabbit, 1:1000, Sigma, A-9196). Final visualisation was completed with the 3,3′-diaminobenzidine reaction (DAB Kit, DAKO). Laser microdissection of immunopositive or immunonegative cells was performed with a Leica AS LMD microscope (Leica, Vienna, Austria) and captured cells placed in an RNase-free PCR cap. PCR was performed on single cells or on

Table 1. Primers (5′→3′) used for qPCR validation of targets from array dataset.

Gene	Forward	Reverse
Gypa	GCATGGGTGAAAGCGTTAGT	GCCACAAAGCCTCTGAGTTC
Gypc	CCCCTCAGCTGTGCTATCTC	CCCTACAACATTCGGAGGAA
Sparc	GAGGGCCTGGATCTTCTTTC	CACGGTTTCCTCCTCCACTA
Vamp1	CTCCTCCCAACATGACCAGT	ACTACCACGATGATGGCACA
Vamp5	CCAAGACTTTAGCCCAGCAG	CTCGGAAGAAAGACGACCAG
Vamp8	CCTCCGAAACAAGACAGAGG	ACAGGGACTGAGCAGCACTT
Tfrc	TCGCTTATATTGGGCAGACC	CCATGTTTTGACCAATGCTG
Abca2	CATCTTGTGTGGCAACAACC	AAGCTTCGGATCTCTGTGGA
Abca4	AGGGAGAGCTGTGGTTCTCA	AGCAAGTCGTCCTTTGGAGA
Abca5	GGACAAATTCAGCCTTTCCA	GAAAGACTTGCGGCTACCAG
Abca7	GTTCTCTGGAGCTGGTTTCG	CAGGGCTGAGACTGTTGTCA
Abcb2	CAGAGAACCTGGGAGCAAAG	CACAACGCCACATAAACCAG
Abcb3	CCTGCCTTTCCTCATAGCTG	CCTGTCTTGGTCTCCTGGAA
Abcb6	CTGGCTGACATCATCATTGG	CGAAACTTGGCTCTCCACTC
Abcb9	GCGGTATTTTCACCCTCGTA	GCGGTTCTCATCAAAGAAGC
Abcc1 (MRP)	CCCAGTGGGAACCTAGTGAA	CTGACTCCCAGCAAGGTCTC
Abcg2 (BCRP)	TCACTGACCCCTTCCATCCTC	AATCCGCAGGGTTGTTGTAG
Abcg5	GTCCTGCTGAGGCGAGTAAC	GCAGCATCTGCCACTTATGA
Abcg8	CCTCCGATTGCTTCTTTCAG	GGCAATCAGAGTCAACAGCA

Table 2. List and characterisation of antibodies.

Immunogen	Manufacturer Species/Type Catalogue Number	Dilution/ Application	Characterisation	Controls
Mouse albumin	abcam Goat/Polyclonal 1° ab19194	1:1000/IHC	Stains expected band of M_r 69×10^3 on Western blot of whole mouse plasma.	Staining abolished after pre-incubation with purified mouse albumin.
Purified full length human Glycophorin A protein	abcam Rabbit/Polyclonal 1° Ab35032	1:10000/IHC	Stains expected band of M_r 40×10^3 on Western blot of whole mouse plasma and kidney tissue extract.	Staining abolished after pre-absorption with mouse plasma.
Recombinant full length human SPARC protein	abcam Rabbit/Polyclonal 1° ab14174	1:10000/IHC	-	Staining abolished after pre-absorption with human plasma.
Recombinant SPARC expressed in human embryonic kidney line HEK-293	Chemicon (Millipore) Rabbit/Polyclonal 1° AB1858	1:100/IHC 1:2500/IHC 1:400/WB	Stains expected band of M_r 34×10^3 on Western blot of whole mouse plasma and kidney tissue extract (see **Fig. 4D**).	Staining abolished after pre-absorption with kidney tissue extract.
Purified immunoglobulin fraction of rabbit antiserum (total plasma protein)	DAKO Rabbit/polyclonal 1° Z0177	1:2000/IHC	Reacts with mouse serum proteins (crossed immunoelectrophoresis) – at least 25 immunoprecipitates appear after staining with Coomassie Brilliant Blue (supplier bulletin).	Staining abolished after pre-incubation with mouse serum.
Immunoglobulins, mainly IgG, isolated from rabbit serum	DAKO Swine/polyclonal 2° Z0196	1:200/IHC	-	-
Purified polyclonal IgG prepared from pooled mouse serum	DAKO Rabbit/polyclonal 2° Z0259	1:200/IHC	-	-
	DAKO Rabbit/polyclonal 2° Z0228	1:200/IHC	-	-

Abbreviations: 1°, primary antibody; 2°, secondary antibody; IHC, immunohistochemistry; WB, western blot.

doi:10.1371/journal.pone.0033554.t002

groups of 2–5 cells (negative controls). Extracted total RNA was directly transcribed into cDNA using the High Capacity RNA-to-cDNA master Mix (Applied Biosystems). PCR was performed using the smallest available intron-spanning TaqMan Gene Expression Assay (with amplicons <100 bp, Applied Biosystems) for *Sparc* (assay ID: Mm00470030_ml), *Glycophorin A* (*Gypa*, assay ID: Mm00494848_ml) and *Glycophorin C* (*Gypc*, assay ID: Mm00503602_ml). Amplification efficiency of the house-keeping gene *hypoxanthine-guanine phosphoribosyltransferase* (*Hprt*, assay ID: Mm01545399_ml) was used as an internal control. PCR products were separated on an agarose gel and stained with ethidium bromide.

Immunocytochemistry

Total protein and albumin staining – cell counting. Selected 5 μm paraffin-embedded sections were dewaxed by heating to 60°C and immersion in histolene, rehydrated through graded alcohols and incubated with Peroxidase and Protein blocking agents (DAKO) for 2 hours each in a moist chamber at room temperature. After washing in PBS+Tween20, sections were incubated in an antibody against mouse serum raised in rabbit (1:2000; DAKO, Z0177) or against mouse albumin raised in goat (1:1000; abcam, ab19194) overnight at 4°C. The following day, sections were washed in PBS+Tween20 and incubated in appropriate secondary antibody (see **Table 2**) for 2 hours. A final incubation in species-specific peroxidase anti-peroxidase (1:200) for 2 hours at room temperature was completed before antibodies were visualized with DAB (DAKO) for 5 minutes. The reaction was halted distilled water, before sections were dehydrated through graded alcohols and mounted with Ultramount #4 mounting medium (Fronine,

Melbourne, VIC, Australia). Positive staining was recognised as a brown colour. Negative control sections included those where the primary antibody was omitted; these always appeared blank. Antibody dilutions were made in PBS-Tween20 buffer with 0.2% fish gelatine (Sigma).

Cell counting was performed on total plasma protein and albumin stained sections. Data are provided in **Table S1**.

SPARC and Glycophorin A immunocytochemistry. In some experiments sections were deparaffinised in xylene, rehydrated through graded alcohols, treated with a 0.5% solution of hydrogen peroxide in methanol for 15 minutes to quench endogenous peroxidase and then rinsed in TRIS buffered saline (TBS, 5 mM Tris-HCl, 146 mM NaCl, pH 7.6). Non-specific binding was inhibited by incubation for 30 minutes with blocking buffer (ChemMate antibody diluent S2022, DAKO) at room temperature. The sections were then incubated overnight at 4°C with one of two rabbit polyclonal antibodies against human SPARC (1:10000; abcam, ab14174; or 1:2500; Millipore/Chemicon, AB1858, see **Table 2**) or a rabbit polyclonal antibody against human GYPA (1:10000, abcam, #35032). The two antibodies against SPARC gave similar appearances however the abcam antibody gave better definition of the reaction product. The sections were washed with TBS and incubated for 30 minutes with a peroxidase-labelled polymer conjugated to goat anti-rabbit/mouse immunoglobulins (EnVision™+ System/HRP K5007, DAKO). The sections were washed with TBS, followed by incubation for 6 minutes with DAB chromogen solution. Positive staining was recognized as a brown colour. The sections were counterstained with Mayer's haematoxylin and dehydrated in graded alcohols followed by xylene and coverslipped with DPX

mounting media (Merck, Darmstadt, Germany). Antibody dilutions were made in blocking buffer (DAKO). Negative control sections were prepared by omitting the primary antibody and always appeared blank. Positive control sections were of mouse kidney (supplier technical bulletin and [32,33] and were always positive.

Western blot

To prepare samples for western blotting analysis, equal weights of plexus tissue were defrosted on ice and mixed with 20 µl PBS (with 0.2% Tween20) before disrupting with a glass mortar and pestle. Tissue was then centrifuged (3 minutes at 900 g, 4°C) to pellet excess cellular debris. Tissue homogenate (10 µl) was mixed with 2.5 µl sample buffer (0.5 M Tris-HCl, 0.4 M glycerol, 0.2 M β-mercaptoethanol, 10% w/v sodium dodecyl sulphate (SDS), 0.5% bromophenol blue, in distilled water). Samples were loaded on 10% Tris-HCl polyacrylamide gels (BioRad, Gladesville, NSW, Australia), with 4 µl of Kaleidoscope Molecular Weight Standard (BioRad). Gels underwent electrophoresis at constant voltage (100 V) in running buffer (25 mM Tris base, 192 mM glycine, 0.1% w/v SDS) for approximately 40 minutes, washed in cold Towbin buffer (25 mM Tris base, 192 mM glycine, 20% w/v methanol; [34]) and transferred at 200 V for 60 minutes to polyvinylidene difluoride membranes (BioRad). Membranes were blocked in a blocking solution of Towbin–Tween buffer (0.1 M Tris, 1.5 M NaCl, 0.1% Tween 20) with 50% low-fat soy milk overnight at 4°C. Membranes were probed using antibodies to mouse SPARC (1:400, Millipore/Chemicon, AB1858) or antibodies to mouse GYPA (1:500, abcam, ab20057), both raised in rabbit. Antibodies were diluted in blocking solution (see above). Incubation with primary antibody was for 2 hours at room temperature. Following washing in Towbin–Tween buffer, membranes were incubated with swine anti-rabbit immunoglobulins (1:500, DAKO, Z0196) for 2 hours at room temperature. Membranes were washed and incubated for a further 2 hours with rabbit peroxidase anti-peroxidase (1:500, DAKO, Z0113). After washing, specifically bound antibody was detected using DAB tablets dissolved with urea (DAB Plus kit, Sigma). The reaction

was stopped in distilled water and membranes dried overnight before being photographed. Kidney was chosen as a control tissue as both SPARC and GYPA are known to be present in this organ [32,35].

A list of all antibodies used in immunohistochemical, western blot and single-cell PCR methods is provided in **Table 2**.

Statistical analysis

For statistical analysis InStat3 software (GraphPad, La Jolla, CA, USA) was used to perform Student's *t*-test and one-way ANOVA (Dunnett or Tukey post-hoc test) as appropriate.

Results and Discussion

In order to identify different macromolecular transporters and changes in gene expression at the blood–CSF barrier in mouse development, Affymetrix GeneChip analysis was used to compare gene expression in choroid plexus collected from embryo versus adult mice. A previously described cell-counting method was used to ascertain the number of total and protein positive epithelial cells in the lateral ventricular choroid plexus of the mouse [18,21,36]. These data (provided in **Table S1**) were used to determine which age had the highest percentage of plasma protein positive choroid plexus epithelial cells to be compared with the adult in a microarray screen, thus E15 was chosen for comparison with adult. Lateral choroid plexus was chosen as this is the tissue on which most of the previous data on protein transfer are available [15,16,18,21].

Microarray results

In total, 23239 probe sets displayed positive hybridization to the Affymetrix GeneChip. The relative gene expression in the plexus is graphically represented by a dot plot (**Fig. 2A**), where each dot represents a single probe set on the Affymetrix GeneChip, with the X and Y logarithmic axis representing the two ages used in the study. From this analysis the bulk of the genes expressed in the lateral ventricular choroid plexus lies near the diagonal axis, indicating that the expression levels do not differ between the two
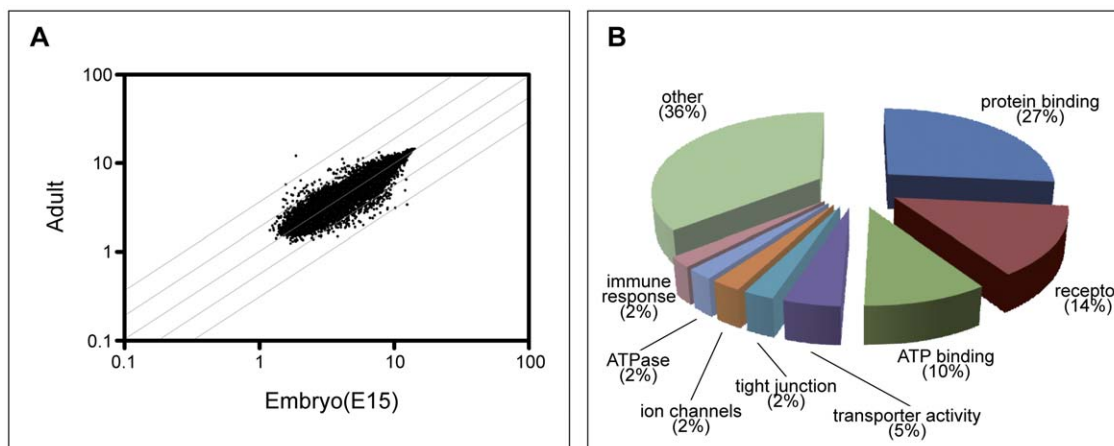

Figure 2. Gene expression in lateral ventricular choroid plexus of E15 and adult mice. A. The data are presented in a dot plot on a logarithmic scale, where each point represents a separate probe set on the GeneChip. Only probe sets that hybridized are represented, with no absent probe sets present in the plot. Data presented in plot are representative of a single GeneChip experiment, however three biological replicates were completed. Probe sets lying on the diagonal axis indicate similar levels of expression at E15 and adult. Validation using qPCR was completed on a select number of targets (see **Fig. 3** and **4**). **B.** Pie chart of the percentage of gene ontology of 1803 genes with altered expression in mouse lateral ventricular choroid plexus between the two ages. Protein binding, receptors and ATP binding genes accounted for 50% of all genes altered during development.
doi:10.1371/journal.pone.0033554.g002

ages (i.e. fold change ≤2). Genes lying on or near this line were not included in further analysis, as the current study was focussed on describing those genes with altered expression in development. However, the large population of genes that did not significantly change their expression indicates a high degree of developmental maturity of the plexus even as early as E15 (three days after the lateral ventricular plexus first begins to develop). The number of probe sets that displayed changes in expression that were 2-fold or higher was 1805, of which 925 were enriched at E15 and 880 were enriched in the adult (see **Table S3**). The top 50 enriched genes are listed in **Table 3**. More stringent discrimination was applied to the gene list using GoMiner™ software (Application Build 253; [30]). Criteria were applied to identify gene targets according to their biological process, molecular function (transporter activity, receptor or vesicle-mediated transport, ion channel, ATPase, ATP-binding) or cellular component (tight junction, plasma membrane). We have previously suggested the presence of putative plasma protein-binding molecules at the blood–CSF barrier [17,20,22], therefore additional classification using molecular function (protein binding) was also carried out. Following classification into these broad biologically coherent categories, several classes of genes with altered expression in development were identified: cell adhesion (118 targets, **Table S4**), ion transport (101 targets, **Table S5**), solute carriers (56 targets, **Table S6**), efflux transporters (181, **Table S7**) and the largest group - protein binding (480 targets, **Table S8**, see also **Fig. 2B**). The relevant functional data sets are available as **Tables S4, S5, S6, S7, S8**. This report will concentrate on genes known to be associated with brain barrier function: tight junction and cell adhesion molecules, ion and water channels, efflux and influx transporters (especially potential protein transporters).

Cell adhesion and tight junction genes

Tight junctions form the structural basis of the blood–brain and blood–CSF barriers [9,37]. The physiological function of tight junction complexes in restricting paracellular diffusion between blood and the CSF is present very early in development [38,39]. Key ultrastructural components such as the number and complexity of protein strands that make up the junction have been shown not to change significantly between very early gestation and adult [40]. Many of the typical proteins found in tight junctions such as ZO-1, occludin and claudins 1, 3–18 and 23 were present in the GeneChip array screen of mouse lateral ventricular choroid plexus. Their expression was similar at E15 and adult (**Table 4** and **Table S4**). *Cldn2* (Claudin 2) and several junctional transmembrane molecules, cytoplasmic adaptors and regulatory small GTPase transcripts did show an age-dependent enrichment in the lateral ventricular choroid plexus (**Table 4**). In particular, *Cldn2* was up-regulated 4-fold in the adult plexus. In contrast, in the embryo, the junctional adhesion molecule *Jam3*, proposed to be an integral part of tight junction complexes, displayed a 3-fold higher expression. The higher expression of *Jam3* in the developing plexus is important as this protein has been implicated in the establishment of the earliest cell-to-cell contacts that even precede tight junction formation [41]. The *Racgap1* (Rac GTPase activating protein 1), also important for the establishment of junctions, was enriched 16-fold at E15. Rac-1, in general, is a major regulator of barrier function and its activation is important for tight junction formation, which along with activation by Tiam1 controls tight junction biogenesis by binding to and activating the Par polarity complex [42]. Additionally, *Cdh2* (cadherin-2/N-cadherin) and *Cdh11* (cadherin-11), both up-regulated in the embryonic choroid plexus (**Table 4**) appear to be important in delineating compartments in the embryonic brain [43,44] but

have not previously been identified in the choroid plexus. *Pcdh18* (protocadherin-18, 6.8-fold increased expression in the embryo) is involved not only in cellular migration during development, but also in cell adhesion [45].

In the adult *Igsf5* (immunoglobulin superfamily 5/Jam4) was up-regulated nearly 10-fold (**Table 4**). The function of this adhesion molecule is dependent on simultaneous expression with other proteins such as Occludin, ZO-1 and Magi1 (membrane associated guanylate kinase with inverted domain structure-1) and were identified in the array screen but displayed no enrichment at either age. Occludin, Marveld2 (tricellulin) and Marveld3 are involved in stabilisation of tight junctions; transcripts for all 3 were detected, but only Marveld3 was differentially regulated (up 4.2-fold in the adult plexus). Although important for the stabilisation of tight junctions, lower expression of Marveld3 is reported not to disturb junction formation but does increase the trans-epithelial electrical resistance in cultures of epithelial cell lines [46], suggesting that Marveld3 may also be important for mediating paracellular ion permeability.

Genes coding for other intracellular accessory tight junctional proteins such as *Dlgh1/5*, *Mpp1/5/6/7*, and *Mpdz* were present in the embryo and showed no change in expression level compared to adult. These intracellular proteins are important components of the tight junction complex structure for two reasons: firstly they anchor the junction to the cytoskeleton; and secondly they may help to regulate the overall function of the structure [38]. Though these molecules are important for junction integrity they are not definitive for the barriers of the brain, but are more broadly components of tight junctions throughout the body [38]. The specific brain barrier accessory proteins *Pard3* and *Cingulin-like 1* (*jacop*) described by Daneman et al. [2] were unchanged in the lateral ventricular choroid plexus in development. This expression of these tight junction–specific molecules at E15 supports the previously described physiological and EM studies demonstrating functional maturity of the blood–CSF barrier even in very early developing brain [39].

The kinesin family member protein, *Kif11*, essential for moving vesicles and organelles within cells along microtubules, was increased 8-fold in the embryo compared to the adult, which could point to a greater importance of these intracellular transport mechanisms in the embryo. Other family members, *Kif2c* (important for removal of tubulin dimers from microtubules), *Kif20a*, *Kif22* and *Kif23* were all up-regulated in the embryo, 7.3-, 5.5-, 4.0- and 4.0-fold respectively. Both *Kif11* and *Kif2c* are highly ATP-dependent, in line with the highly metabolically active nature of these cells. These genes may be important in mechanisms that involve vesicular transport (see below).

Ion transporters and channels

A key component of the internal environment of both the adult and developing brain is the stability of the ionic composition of the CSF, which is usually assumed to reflect that of brain interstitial fluid. The ionic composition of CSF in developing brain is different from the adult. Some CSF/plasma gradients are established very early in development, indicating the integrity of tight junctions is already restricting paracellular pathway diffusion of ions and that there are active ion pumps in the plexus epithelial cells (see [9] for summary). In the adult, the key mechanisms involved in CSF secretion are carbonic anhydrase, which generates HCO_3^- that is transported across the epithelial cells and the sodium-potassium exchanger (Na+/K+ ATPase) in the apical membrane of the plexus epithelial cells [47]. In fetal rat choroid plexus the levels of carbonic anhydrase and Na+/K+ATPase are known to be much less than in the adult [8].

Table 3. Top 50 genes enriched in the embryonic (A) or adult (B) lateral ventricular choroid plexus of the mouse.

(A) Gene	GenBank ID	Fold Change	(B) Gene	GenBank ID	Fold Change
H19	BC025150	81.0	Prlr	BC096586	234.3
Slc16a10	BC052877	66.8	Agxt2	M22959	97.1
Gpc3	BC036126	60.4	Cox8b	BC086930	28.8
Ddx3y	BC021453	24.1	Kl	AB005141	27.4
Rspo2	NM_172815	19.3	D12Ertd647e	BC128276	25.3
Hist1h1b	NM_020034	17.6	Scd1	BC007474	24.1
Ccna2	BC052730	17.1	Tgfb2	BC011170	18.5
Igf2bp1	BC051679	16.6	Hist1h2bc	BC019673	18.3
Racgap1	AB030252	16.0	Maob	BC113788	17.9
Sulf2	AK129316	15.9	Inmt	BC013518	17.8
Abcg5	AF312713	14.1	Cpxm2	AF017639	16.4
Ccdc67	BC096547	13.1	Npal2	BC030399	15.5
4930579J09Rik	AY032666	12.8	Sod3	U38261	14.8
Ppic	M74227	12.1	Sult1c2	AY005469	14.5
Slc6a15	AY149280	11.4	Ltc4s	U27195	14.2
Bex1	BC058805	11.3	Slc5a5	AF235001	13.6
Tpx2	BC060619	11.2	Tmem184a	BC026659	13.3
Fscn1	BC052408	11.1	Ppp2r2c	BC059811	13.1
Nrk	AB020741	10.7	Sytl2	AB057754	12.3
Rassf4	BC060709	10.6	F5	U52925	11.7
Prom1	AF039663	10.6	Sfrp5	BC032921	11.7
Tmem26	BC117502	10.3	BC055107	BC055107	11.1
Prc1	BC059808	10.0	Steap1	BC061023	10.8
Asb4	BC046819	9.7	Chdh	BC039186	10.8
Slc40a1	AF231120	9.6	Il1r1	M20658	10.2
Wfikkn	AY308804	9.6	Acsl6	AY786360	10.2
Rspo3	AB055811	9.4	Pla2g5	AF162713	10.2
Cdc2a	U58633	9.2	Ccl9	U15209	10.2
Gli3	NM_008130	9.1	Plek2	AF170564	10.1
Gdf5	U08337	9.0	Abca4	AF000149	9.7
Col3a1	BC043089	8.8	Rdh5	AF033196	9.7
Fn1	BC051082	8.7	Scx	BC062161	9.6
Plk1	L19558	8.6	Slc39a4	BC023498	9.6
Crabp2	M35523	8.6	Klf9	Y14296	9.6
Pbk	BC020099	8.5	Rrh	BC046288	9.6
Bub1b	AF107296	8.4	Igsf5	BC004806	9.6
Kif11	BC060670	8.2	Lrrtm2	AY182027	9.4
Kit	BC052457	8.1	Ppp1r1b	BC011122	9.3
Fstl1	M91380	7.9	Crhr2	U19939	9.0
A230106N23Rik	BC116972	7.9	Cd74	BC096435	9.0
Calcrl	AB015595	7.8	Nos1	D14552	8.9
Ccnb2	BC008247	7.7	Kcnh1	U04294	8.9
Sema6a	BC059238	7.7	Bdkrb1	BC120684	8.8
Pnck	AF181984	7.7	Car5b	AF192978	8.7
Ctnna2	BC079648	7.6	Gabrb1	BC130258	8.6
Col4a1	J04694	7.5	Slc41a2	NM_177388	8.5
Mfap2	L23769	7.5	Gpr37l1	AB016602	8.5
Cercam	D16263	7.5	Me3	BC099935	8.4

Table 3. Cont.

(A) Gene	GenBank ID	Fold Change	(B) Gene	GenBank ID	Fold Change
Casp7	D16263	7.5	Sult4a1	BC054757	8.4
Vcan	BC115766	7.4	Aox1	AB017482	8.4

The top 50 most enriched lateral ventricular choroid plexus-specific gene targets in the embryo (**A**) or adult (**B**). Fold change column represents the increases in the number of transcripts for each gene compared to levels in opposing age (eg. a fold change of 3.0 for an embryonically enriched gene has expression 3-times higher than the adult). For full data set, refer to **Table S3**.
doi:10.1371/journal.pone.0033554.t003

Similar results were obtained in the present study (**Table S3**). Thus the alpha subunit of the Na+/K+ATPase (*atp1a2*) was up-regulated in the adult over 7-fold: similarly, the carbonic anhydrases (*CA5b, CA8, CA13*) were up-regulated 4- to 9-fold in the adult (**Table S3**).

In the adult there was also enrichment in potassium ion channels (*Kcnh1, Kcnd3, Kcnd3, Kcnh2* and *Kcnk1*) ranging from 3 to 8-fold of levels seen at E15 (**Table 5**), while very few potassium-only ion channels showed increased expression in the embryo (though *Trpm5*, a potassium, sodium, caesium and calcium ion channel was 6.9 fold enriched, **Table 5**). The major extracellular cation, sodium, is transported by a number of solute carrier (*Slc*) gene products. Some were enriched in the embryo (*Slc6a13* – 4.6-fold, *Slc4a4* – 4.1-fold) and others in the adult (e.g. *Slc5a5* – 13.6-fold; *Slc24a4* – 7.8-fold, **Table 5** and **Table S5**). Anion transporters are also fundamental components for maintenance of the internal environment of the brain as well as CSF secretion, in particular Cl$^-$ and HCO$_3^-$. Anion transporters known to be important in adult choroid plexus belong to the Slc4 family

Table 4. Tight junction and associated proteins enriched in mouse lateral ventricular choroid plexus.

(A) Gene	GenBank ID	Fold Change	(B) Gene	GenBank ID	Fold Change
Transmembrane					
Pcdh18	BC052198	6.9	Igsf5	BC004806	9.6
Cdh5	BC054790	4.3	Cldn2	BC085494	4.3
Cmtm3	AY241870	4.0	Marveld3	BC025851	4.2
Cdh2	AB008811	3.4	Cldn12	BC024057	2.1
Jam3	BC024357	3.2			
Cldn11	BC021659	2.0			
Cytoplasmic Adaptors					
Asb4	BC046819	9.7	Ankrd57	NM_172939	4.9
Ctnna2	BC079648	7.6	Ank	DQ832285	3.3
Lama4	U59865	6.7	Lin52	BC048485	3.2
Arhgap11	AK129034	5.7	Prkcz	BC072590	3.0
Dlg7	AB076696	5.5			
Cdh11	BC046314	3.7			
Regulatory Adaptors					
Racgap1	AB030252	16.0			
Rhobtb3	AK129234	4.6			

List of proteins known to be associated with tight junctions that were up-regulated in either the embryo (**A**) or the adult (**B**) expressed as fold change compared to levels in other age. A full list of gene products involved in cell adhesion can be found in **Table S4**.
doi:10.1371/journal.pone.0033554.t004

[46,47]. Two that were up-regulated in the embryonic choroid plexus are *Slc4a1* (Cl$^-$-HCO$_3$ exchanger) and *Slc4a4* (Na$^+$-HCO$_3^-$ co-transporter) see **Table 6**. No functional studies on individual ion transporters in developing brain or choroid plexus have been published, but it is possible to infer ion transport function from studies of CSF and plasma ion composition in the developing brain. Ion gradients between CSF and plasma are a characteristic of brain homeostasis [48]. Some ion gradients are established very early in brain development, for example Cl$^-$ in fetal sheep [49] and neonatal rats [50]. This indicates that ion transport mechanisms are functional early in brain development, indicating functional activity of the ion transporters expressed in developing choroid plexus.

Aquaporins

Aquaporins 1–9, 11, 12 were all expressed at similar levels in both embryonic and adult choroid plexus epithelial cells (**Table S2**). Only Aquaporin 1 has been established as having a clear function in water transport and CSF secretion in the choroid plexus [45]; it has previously been shown that this water channel is demonstrable immunohistochemically as soon as the choroid plexus differentiates and the expression level, as determined by real time RT-PCR did not change between E14 and adulthood [51].

Amino acid influx transporters

Numerous members of the solute carrier gene family (*Slc*) of membrane transport proteins were present in the choroid plexus (**Table 5**, **Table 6** and **Table S6**). This large family (with over 300 members) is involved in the transport of many solutes across cellular membranes, and include ion channels and aquaporins (see above) facilitative transporters and active transporters. Three categories of expression of solute carriers were found in the developing mouse choroid plexus: those enriched in the embryo, those enriched in the adult, and those with relatively high expression levels that did not change with development. At E15, the mouse lateral ventricular choroid plexus contained many carriers involved in the transport of amino acids: *Slc16a10* (67-fold increase), *Scl7a11* (7-fold) and *Slc1a4*, *Slc38a4* and *Slc7a1* (all approximately 4-fold). These are summarised in **Table 6**. The transport of amino acids into the CSF and the developing brain is important for normal development. Most are directly involved in protein metabolism underlying cellular growth of the brain. Some are important because they act as carriers, for example, thyroid hormone transporters. The main ones so far described, *Slc16a2* (MCT8) and *Slco1c1* (Oatp14), have recently been identified in cerebral endothelial and choroid plexus epithelial cells of rat fetuses [52]. In the present study the expression levels of these transports were similar in E15 and adult choroid plexus, as were many other transporters in the MCT and Oatp families (**Table S3**). Another thyroid hormone transporter *Slc16a10* (TAT1, MCT10; [52]) showed strikingly high expression in embryonic

Table 5. Influx transporters and ion channels enriched in mouse lateral ventricular choroid plexus.

(A) Gene	GenBank ID	Fold Change	(B) Gene	GenBank ID	Fold Change
Solute Carriers					
Slc16a10	BC052877	66.8	Slc5a5	AF235001	13.6
Slc6a15	AY149280	11.4	Slc39a4	BC023498	9.6
Slc40a1	AF231120	9.6	Slc41a2	NM_177388	8.5
Slc7a11	AY766236	7.1	Slc24a4	AY156046	7.8
Slc4a1	BC053429	5.5	Slc28a3	BC013783	6.9
Slc6a13	BC029637	4.6	Slc24a5	AB085629	6.1
Slc1a4	BC043483	4.4	Slc9a7	BC058750	5.8
Slc38a4	AY027919	4.2	Slc6a17	AY155578	3.5
Slc6a6	L03292	4.1	Slco1c1	AY007379	5.2
Slc4a4	AF141934	4.1	Slc4a10	AK220501	5.0
Slc7a1	M26687	4.1	Slc39a14	AB177995	4.0
Slc39a8	BC006731	3.3	Slc35f3	BC115965	3.9
			Slc13a4	BC089161	3.9
			Slc37a2	AF121081	3.5
			Slco1a5	AF240694	3.4
			Slc39a12	BC089362	3.3
			Slc46a1	BC057976	3.2
			Slc25a35	BC019996	3.1
			Slc22a5	AF110417	3.0
Ion Channels					
Racgap1	AB030252	16.0	Steap1	BC061023	10.8
Trpm5	AB039952	6.9	Kcnh1	U04294	8.9
Myb	M12848	6.5	Gabrb1	BC130258	8.6
Kcnip1	AY171234	5.3	Gabra4	BC094603	7.9
Gabrg	BC099939	3.8	Atp1a2	BC036127	7.7
Cngb3	AJ243572	3.7	Trpv4	AF279672	7.6
Ttyh3	BC062917	3.6	Chrnb4	AF492840	6.9
Gabra3	M86568	3.4	Nwd1	BC024788	6.3
Fxyd6	BC051127	3.3	Cacnb4	BC026479	6.4
			Slc9a7	BC058750	5.8
			Atp2a3	BC026147	5.7
			Atp13a4	BC048410	5.6
			Dmpk	BC075715	5.4
			Kcnd3	AF107781	5.4
			Trf	BC092046	5.1
			Pln	BC061097	4.7
			Best3	AY450426	3.7
			Kcnh2	AF012868	3.5
			Atp1b1	BC094070	3.3
			Kcnk1	AF033017	3.2

Solute carriers and ion channels up-regulated in either the embryo (**A**) or the adult (**B**). In total, 157 targets were found for these gene ontology categories, with only those targets with fold change >3.0 shown above. A comprehensive list is presented in **Table S5, S6**.
doi:10.1371/journal.pone.0033554.t005

Table 6. Expression and function of transporters in developing choroid plexus.

Transporter	Fold Change	Transport Function	Reference
Slc16a10	66.8	iodothyronines T3, T4	[92]
Slc6a15	11.4	neutral amino acids	[57]
* Slc40a1	9.6	iron	[93]
Slc7a11	7.1	cysteine, glutamate	[57]
Slc4a1	5.5	anion transporter, (Cl^--HCO_3 exchange)	[46,49]
Slc6a13	4.6	GABA transporter	[94]
Slc1a4	4.4	glutamate, neutral amino acids	[95]
Slc38a4	4.2	acidic & neutral amino acids	[57,95]
Slc6a6	4.1	taurine	[57]
Slc4a4	4.1	Na^+-HCO_3^- cotransporter	[46]
Slc7a1	4.1	acidic amino acids	[57]
Slc39a8	3.3	zinc transporter	[96]

The expression levels for the transporters listed were obtained from Affymetrix array analysis of E15 and adult mouse choroid plexus. Only Slc4a4, Slc7a11 and Slc40a1 have previously been identified in choroid plexus. Fold change in expression compares E15 to adult choroid plexus. Superscript numbers indicate published studies showing transport into developing brain or CSF.
*Gene product ferroportin-1 identified in choroid plexus.
doi:10.1371/journal.pone.0033554.t006

membrane sorting and recycling [54]; its expression in developing choroid plexus may be relevant to the protein transport mechanisms discussed below.

Direct measurement of amino acid transport in the brains of newborn animals has previously shown that many amino acids are indeed transported to a higher degree than in the adult [55–58]. This was supported by the finding in our study of enrichment of a large number of amino acid transporters at E15 (**Table 6**). In contrast, in the adult only one solute carrier responsible for the movement of amino acids was up-regulated (Slc6a17), although many more were actually present, either in levels not differing from the embryo, or less than at E15. **Table 6** indicates the available information on function of these transporter mechanisms in the developing brain; it is not yet possible to link directly the expression and transport function of individual genes in the developing brain. This is partly because many of the genes have only been identified recently, but also because of redundancy, the current experimental evidence is not adequate to define the function of individual genes. These earlier results from studies of amino acid transport are consistent with our overall finding of a higher level of expression of a large number of Slc genes in the embryonic choroid plexus compared to the adult.

Efflux transporters

The ATP-binding cassette (ABC) transporter family has been shown to be a key element of both the blood–brain and blood–CSF barriers from very early in development that can actively efflux a large number of lipophilic drugs [59]. ABC transporters are divided into seven distinct subfamilies: ABC1, multidrug resistance proteins (MDR/TAP), multidrug resistance-associated proteins (MRP), ALD, OABP, GCN20 and White. While many of these could be detected in the present screen of choroid plexus, most did not show evidence of developmental regulation (**Table 7** and **Table S7**). Two efflux transporters, Abcg5 and Abcg8, were up-regulated 14.1- and 3.7-fold respectively at E15 compared to the adult. These have both been detected previously in adult rat

choroid plexus (**Table 6**). However, Slc16a10 has been previously reported as undetectable in the adult brain [53]. TAT1 (Slc16a10, MCT10) has also been proposed to be involved in endocytotic

Table 7. ABC transport/drug efflux gene expression in mouse lateral ventricular choroid plexus.

(A) Gene	Other IDs	array	qPCR	(B) Gene	Other IDs	array	qPCR
Abcb3	TAP2	-	16.5	Abca2		3.5	22.4
Abcb6	UMAT,MTABC3	2.6	8.1	Abca4	ABCR,RP19,RIM	9.7	12.9
Abcg2	BCRP	-	15.8	Abca5		2.5	1.4
Abcg5	Sterolin1,White3	14.1	44.8	Abca7	ABCX	4.5	-
Abcg8	Sterolin2,White4	3.4	20.3	Abcb9	TAPL	2.8	1.8
				Abcc1	MRP,MRP1	2.3	-

(C) Gene	Other IDs	array	(C) Gene	Other IDs	array
Abca1	TGD, CERP	NC	Abcc3	MRP3	NC
Abca3	ABC-C	NC	Abcc5	ARP5	NC
Abca6		NC	Abcc6	MRP6	NC
Abca8a		NC	Abcc9	SUR2	NC
Abca8b		NC	Abcc10	MRP7	NC
Abca9		NC	Abcc12		NC
Abca12		NC	Abcd1	ALD,ALDP	NC
Abca13		NC	Abcd2	ALDL1,ALDR	NC
Abca14		NC	Abcd3	PXMP1,PMP70	NC
Abca15		NC	Abcd4	PXMP1L,P70R	NC
Abca16		NC	Abce1	OABP	NC
Abcb1a	MRD1, P-GP	NC	Abcf1		NC
Abcb2	TAP1	NC	Abcf2		NC
Abcb4	MDR3	NC	Abcf3		NC
Abcb8	M-ABC1	NC	Abcg1	White	NC
Abcb10	M-ABC2,MTABC2	NC	Abcg3		NC
Abcb11	BSEP,SPGP,PGY4	NC	Abcg4	White4	NC
Abcc2	MRP2	NC			

Most enriched genes during development of the mouse lateral ventricular choroid plexus in the embryo (**A**) or adult (**B**). Some genes were present at both ages with no alteration in expression levels (**C**). Data obtained from Affymetrix GeneChip array and qPCR. Array targets were considered enriched with fold changes equal or greater than 2.0. See also **Table S7**. Abbreviations: NC, no change (in expression); -, not tested.
doi:10.1371/journal.pone.0033554.t007

choroid plexus, but only at a low level [58]. Several other ABC transporter genes have been shown to be differentially expressed in developing rat choroid plexus [10]. We found that BCRP (Abcg2) showed a strikingly higher expression in embryonic rat choroid plexus, whereas PGP (Abcb1) was not significantly different and MRP1 (Abcc1) and MRP4 (Abcc4) expression was significantly less in the embryo [10]. In the present study some of these genes were validated in mouse choroid plexus using RT-PCR (**Fig. 3**, **Table 6**). This confirmed that Abcg2 (BCRP), Abcg5 and Abcg8 were substantially up-regulated in the embryonic choroid plexus as were Abcb3 and Abcb6 (**Fig. 3A**). In the adult Abca2 and Abca4 were up-regulated compared to E15 choroid plexus (**Fig. 3B**). The higher expression of BCRP (Abcg2) in the embryonic choroid plexus may be related to the physiologically hypoxic environment in utero [60] as it has been reported that hypoxia causes up-regulation of BCRP [61]. However, these latter findings need to be interpreted with caution, because of the in vitro conditions in which the experiments were conducted (see [6]).

Protein binding

The protein concentration in CSF in the developing brain is higher than in the adult (for review see [14]). It has been suggested that a protein-specific transfer mechanism may regulate movement of some proteins from blood into CSF and that this mechanism could be receptor-mediated [16,17,18,20–22]. The physiological importance of high protein concentration in the developing CSF has been proposed to be: (i) maintaining high colloid-osmotic pressure gradients allowing normal brain development; and, (ii) act as a carrier for many essential molecules such as growth factors, hormones or nutrients (for review see [8]). The array dataset obtained in this study was mined for candidate genes with known protein-binding properties. The results are shown in **Table 8 and Tables S2** and **S8**. Three of the targets identified, Gypa, Gypc and Sparc (osteonectin/BM-40/culture-shock protein) were selected for further study because of their reported role in the binding of albumin [62]. SPARC has also been recently reported in the choroid plexus epithelium [22].

Glycophorins are the main sialoglycoproteins of erythrocytes (for review see [63,64]). Although there is evidence that many plasma proteins seem to be transferred from blood into the CSF, albumin has been most extensively studied [9,15,17,20,22]. GYPA and other albumin-binding proteins which are able to facilitate the transcytosis of native albumin in peripheral vascular beds and epithelial tissues have been reported to be virtually absent in adult brain capillaries [62]. Another albumin binding protein, SPARC (osteonectin/BM-40/culture-shock protein), is a soluble protein that can be found either incorporated into the plasma membrane of cells, floating free in the cytoplasm of cells or extracellularly in
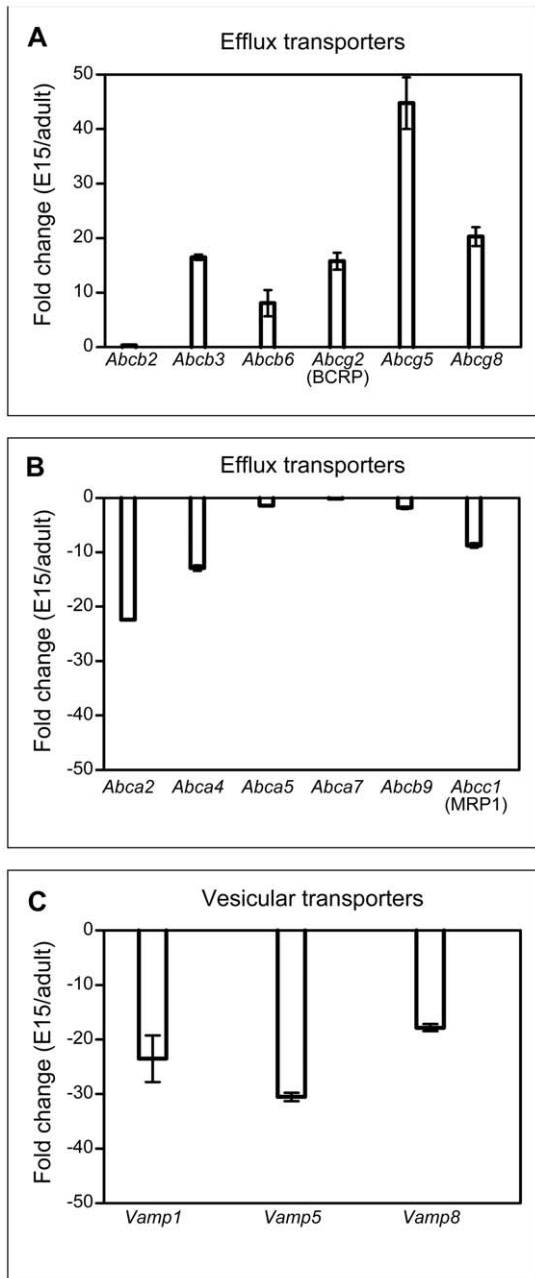
Figure 3. qPCR validation of microarray gene targets. Several members of the ABC family of efflux transporters were up-regulated in the embryo (**A**) and in the adult (**B**). The direction of these changes was in line with what was found using the Affymetrix GeneChip platform, though the magnitude of the expression was different. **C.** Three members of the vesicle-associated membrane protein (*Vamp*) family of proteins were down-regulated in the embryo (up-regulated in the adult).
doi:10.1371/journal.pone.0033554.g003

the blood plasma [65,66]. SPARC is a glycoprotein that has been shown to be involved in protein binding (especially of albumin) in other epithelia [32,35]. It has also been proposed to be a targeting molecule for albumin at the blood–CSF barrier [22] and to modulate cell matrix interactions, inhibit proliferation and affect growth factor signalling, as well as bind calcium and proteins such as albumin [66–71]. SPARC has been found localised to the basement membrane of many cell types [66]. Further analysis was

restricted to targets related to protein transport properties of the choroid plexus.

Both *Gypa* and *Gypc* along with *Sparc* were found to be enriched in the lateral ventricular choroid plexus at E15 compared with the adult (6.1-, 3.7- and 2.2-fold respectively). These changes were confirmed with qPCR (**Fig. 4C**). Antibodies to SPARC and GYPA were used in western blots to estimate the change in levels of the protein present in developing choroid plexus cells. These results are presented in **Fig. 4D** and show that there were higher levels in the embryo than in the adult.

Single cell PCR. To ascertain the cellular co-localisation of albumin and its putative targeting proteins Sparc, Gypa and Gypc, laser dissection of both albumin- and total plasma protein-immunopositive plexus epithelial cells followed by single-cell RT-PCR was performed. The data are shown in **Fig. 4E**. For immunostained cells, 60–80% of albumin-immunopositive plexus epithelial cells showed expression of *Sparc* and both glycophorins at E15. For glycophorin targets this increased to 90–100% in the adult. In contrast, *Sparc*-expression in the adult was only present in approximately 40% of albumin-immunopositive plexus cells. Albumin- and total plasma protein-immunonegative cells of the plexus epithelium did not show amplification signals for either *Sparc* or the glycophorins at any age (**Fig. 4E**). In embryonic choroid plexus, numbers of cells immunopositive for total plasma protein that also showed high *Sparc* expression were higher than those immunopositive for albumin. All of the total plasma protein-immunopositive cells were also positive for both *Gypa* and *Gypc*. In the adult choroid plexus, the number of total plasma protein-immunopositive cells that were also *Sparc*-positive was less than in the embryo. All plasma protein immunostained cells were positive for *Gypa*, but for *Gypc* fewer plasma protein-immunopositive cells were positive than was the case for embryonic choroid plexus. The generally higher proportion of cells immunostained for total plasma protein than for albumin that also expressed these putative transporters indicates that SPARC and GYPA and GYPC are likely to be involved in transport of other plasma proteins, in addition to albumin, across choroid plexus epithelial cells.

Cellular & subcellular distribution of Glycophorin A. In order to investigate the possible role of one of these albumin-binding molecules in transport across the blood–CSF barrier, we have examined the distribution of GYPA at the cellular and subcellular level in lateral ventricular choroid plexus throughout mouse development from E12 onwards (see Methods) using a cross-reacting polyclonal antibody and the EnVision™+ system. Results are illustrated in **Fig. 5**. GYPA was detected in individual choroid plexus epithelial cells of animals at all ages from the first appearance of the lateral plexus at E13 (not shown), with a peak in intensity at E15–E16. Most epithelial cells exhibited weak immunoreactivity at this age but there were some cells, particularly in the older parts of the plexus (upper part of **Fig. 5A**), that showed strong immunoreactivity on the apical (CSF) surface (**Fig. 5A**). There was a marked decrease in immunoreactivity in the adult (**Fig. 5B**). The staining pattern was also different at different developmental ages. At E15 choroid plexus epithelial cells exhibited a predominantly peripheral plasma membrane-associated staining in both epithelial (apical and basolateral cell membrane) and endothelial cells (**Fig. 5A**). In contrast, in adult choroid plexus, immunoreactivity in general was absent from both apical and basolateral choroid plexus epithelial cell membranes, but was present intracellularly at a low level. In a few small segments of the plexus a stronger positive intracellular staining for GYPA was present (framed area in **Fig. 5B**).

At the subcellular level at the youngest ages, E13 and E14, a strong fine granular immunoreactivity for GYPA was present in

Table 8. Protein binding targets enriched in mouse lateral ventricular choroid plexus.

(A) Gene	GenBank ID	Fold Change	(B) Gene	GenBank ID	Fold Change
Hist1h1b	NM_020034	17.6	Kl	AB005141	27.4
Ccna2	BC052730	17.1	Tgfb2	BC011170	18.5
Bex1	BC058805	11.3	Cpxm2	AF017639	16.4
Fscn1	BC052408	11.1	Sod3	U38261	14.8
Rassf4	BC060709	10.6	Sytl2	AB057754	12.3
Wfikkn2	AY308804	9.6	Sfrp5	BC032921	11.7
Cdc2a	U58633	9.2	Il1r1	M20658	10.2
Gli3	NR_027010	9.1	Acsl6	AY786360	10.2
Gdf5	U08337	9.0	Igsf5	BC004806	9.6
Fn1	BC051082	8.7	Lrrtm2	AY182027	9.4
Plk1	L19558	8.6	Crhr2	U19939	9.0
Pbk	BC020099	8.5	Cd74	BC096435	9.0
Kit	BC052457	8.1	Nos1	D14552	8.9
Sema6a	BC059238	7.7	Gabrb1	BC130258	8.6
Ctnna2	BC079648	7.6	Atp1a2	BC036127	7.7
Cercam	NM_207298	7.5	Trpv4	AF279672	7.6
Cntn4	BC115766	7.4	Rnf152	BC118961	7.5
Nek2	BC010302	7.3	Dsg2	AB072269	7.5
Anxa2	BC003327	7.1	Bhlhb2	BC010720	7.3
Cdk6	AF132483	7.0	Cadm2	NM_178721	6.9
Pcdh18	BC052198	6.9	Hopx	AF492703	6.6
Uhrf1	AF274046	6.8	Cish	BC022178	6.5
Lama4	U59865	6.7	Zbtb20	BC056446	6.5
Myb	M12848	6.5	Cd9	BC070474	6.3
Dach1	AF129510	6.2	6330514A18Rik	BC099679	6.2
Col12a1	U25652	6.1	Lynx1	BC037541	6.1
Gypa	BC148192	6.1	Cacnb4	BC026479	6.0
Jarid1d	AF127244	5.8	H2-Aa	BC031711	5.8
Cd93	AF081789	5.7	Pcolce	AB008548	5.8
Nkd1	AF343352	5.6	Plp1	M15442	5.8
Trim59	BC025430	5.6	Tgfa	U65016	5.7
Slc4a1	BC053429	5.5	H2-D1	U47325	5.7
Cadm1	AF434663	5.5	Cltb	BC070404	5.6
Emid2	BC075713	5.5	A2m	BC072642	5.6
Sept11	BC064466	5.2	S100a1	BC005590	5.4
Plk4	L29479	5.1	Kcnd3	AF107781	5.4
Ezh2	BC079538	5.1	Tlr3	BC099937	5.1
Fkbp10	BC029546	5.1	Nfasc	AJ543322	5.1
Ccnb1	BC011478	5.1	Pcolce2	BC051174	5.0
Cited2	BC057126	5.1			
Dnajb13	AF419292	5.1			
Mfap4	BC022666	5.1			

List of protein binding targets that were up-regulated in either the embryo (**A**) or the adult (**B**). In total, 479 targets were found for this gene ontology category, with only those targets with fold change >5.0 shown above. A comprehensive list is presented in **Table S8**.
doi:10.1371/journal.pone.0033554.t008

the apical cytoplasm in the most mature choroid plexus epithelial cells opposite the hippocampal anlage. This segment of the plexus showed a weak staining of the epithelial basal membranes and of endothelial cell surfaces (not shown). The most intense staining was visible at E15 when pronounced membrane-associated GYPA immunoreactivity was visible along the apical surface of epithelial cells of larger segments of plexus (**Fig. 5A**). In the same areas basolateral membranes as well as endothelial cell membranes were also strongly stained (**Fig. 5A**). A few small vesicles in the apical cytoplasm showed reactivity whereas the nuclei were always
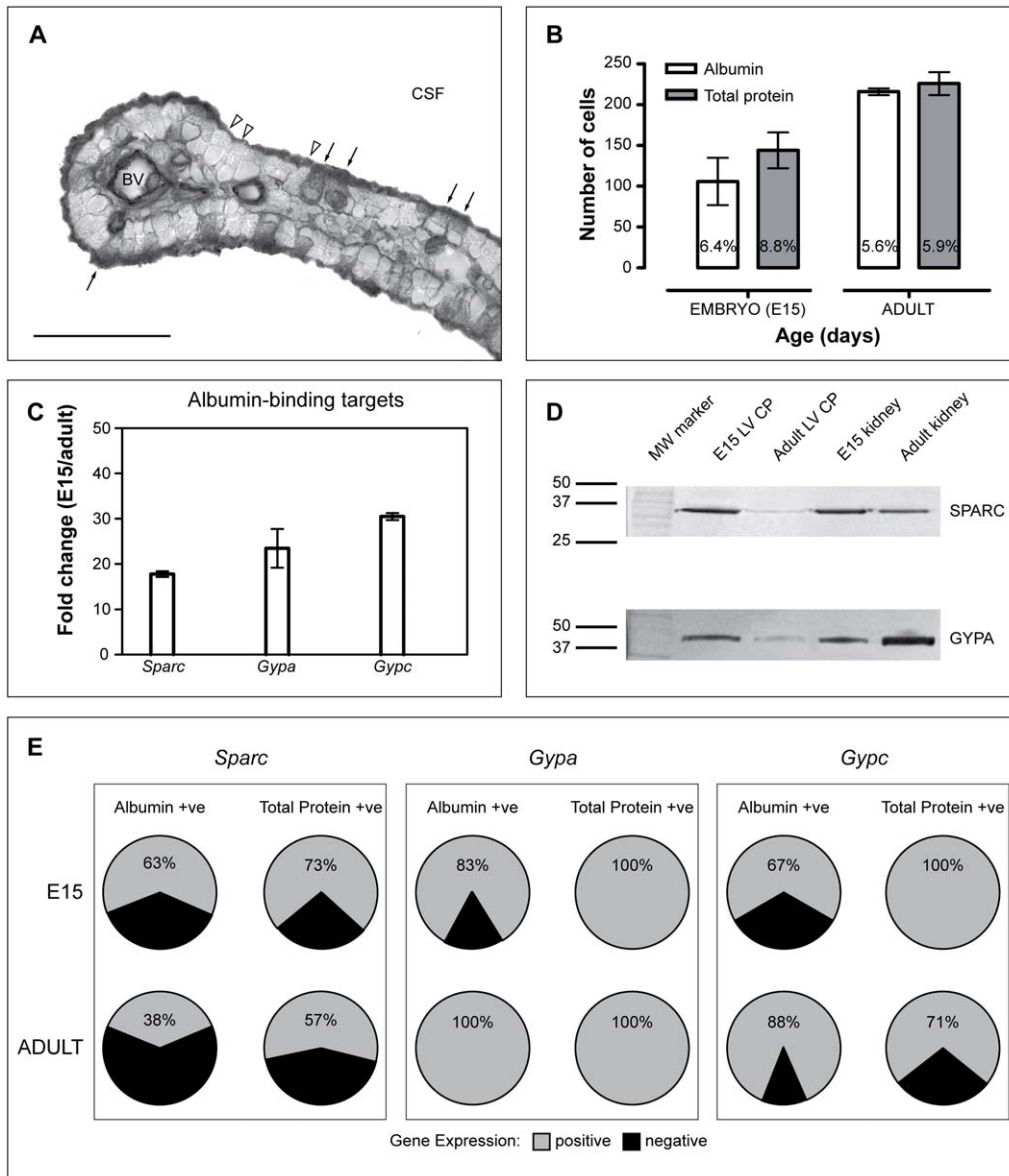
Figure 4. Co-localisation of albumin and total plasma protein with SPARC, Glycophorin A or C. A. Immunoreactivity in the lateral ventricular choroid plexus of E15 mouse embryo immunostained to detect endogenous albumin. Several epithelial cells of the plexus were deemed albumin-immunopositive (filled arrows), while all other cells were albumin-immunonegative (unfilled arrowheads). To be included in cell counts, the reaction product had to be present from basolateral to apical membranes and a cell nucleus had to be visible. **B.** Summary of cell count data from E15 and adult mouse lateral ventricular choroid plexus. The number of both total protein- and albumin-immunopositive plexus cells increased with age. As a percentage (numbers in bars), there was a decrease between E15 and adult, with E15 having the higher percentage of protein-positive cells of any age of the developing mouse. **C.** Quantitative PCR validation of microarray experiments showed that *Sparc*, along with *Gypa* and *Gypc* were up-regulated from about 20- to 30-fold in the embryo compared to the adult. **D.** Western blots of SPARC and GYPA in lateral ventricular choroid plexus and kidney (used as control) of E15 and adult mice. The level of SPARC did not change in kidney at the two ages: there was a substantial decrease in adult lateral ventricular choroid plexus compared to E15. A single dark staining band at the correct molecular weight (~35 kDa, mouse SPARC MW 32 kDa) confirms specificity of the antibody. Levels of GYPA appeared to be higher in the adult kidney compared to E15. The highest level in the choroid plexus was in the embryo. A dark staining band at ~40 kDa (mouse GYPA MW 43 kDa) confirms cross-reactivity of antibody. **E.** Single-cell PCR was performed on cells immunostained for either total protein or albumin. The percentage of immunopositive plexus cells that also displayed positive gene expression increased with age for both glycophorins, however it decreased for *Sparc*. Abbreviations: E, embryonic day; *Gypa*/ GYPA, Glycophorin A; GYPC, Glycophorin C; LV CP, lateral ventricular choroid plexus; MW molecular weight (kDa).
doi:10.1371/journal.pone.0033554.g004

negative (**Fig. 5A**). In the adult a marked decrease in the cell surface–associated epithelial membrane staining was observed (**Fig. 5B**). The cytoplasm exhibited an overall fine granular reactivity, with most immunoreactivity in the basal cytoplasm. A distinct immunostaining of small vesicles (arrows in **Fig. 5B**) was still present. Small segments of the plexus showed a stronger

reactivity (framed area in **Fig. 5B**). There was no reactivity for GYPA in vascular endothelial cell membranes.

Cellular & subcellular distribution of SPARC. Cellular distribution of SPARC at the blood–CSF barrier was also investigated. Results are illustrated in **Fig. 6.** SPARC was detected in individual choroid plexus epithelial cells of animals
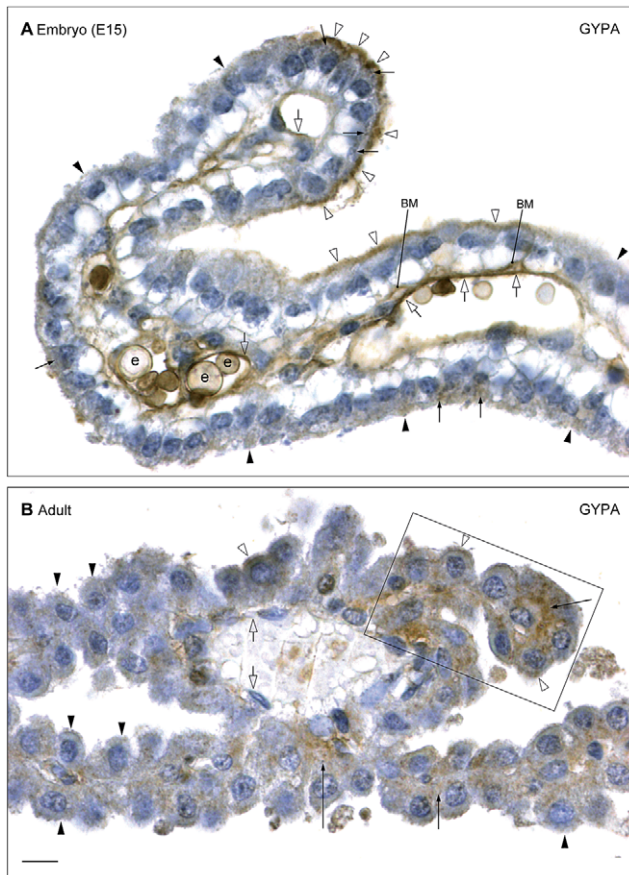
Figure 5. Cellular and subcellular distribution of GYPA immunoreactivity in E15 and adult choroid plexus. A. Embryonic day 15 (E15) lateral ventricular choroid plexus. The more medial younger segment of the plexus emerging from the hem and hippocampal anlage is shown in the lower and right side of the figure. This part of the plexus shows only weak immunopositive staining for GYPA (filled arrowheads). At the tip of the plexus most epithelial cells exhibit a strong granular immunoreactivity in the apical cytoplasm (arrows) and an apical membrane-associated surface immunostaining (open arrowheads). Basolateral cell membranes (BM) are also immunopositive, as are vascular endothelial cells, which show a marked immunoreactivity (open arrows), in particular in areas with basolateral and apical epithelial membrane-associated immunostaining. Strong membrane immunostaining of erythrocytes (e) is also evident. **B.** Adult lateral ventricular choroid plexus. A very weak fine granular cytoplasmic immunoreactivity is seen in almost all choroid plexus epithelial cells in contrast to a stronger immunoreactivity found in few small segments of the plexus (framed area). Note the apparent lack of cytoplasmic immunostaining in the apical-most part of most epithelial cells (filled arrowheads), but a distinct immunostaining of small vesicles within the cytoplasm (arrows). Very few cells exhibit an apical membrane-associated immunoreactivity (open arrowheads). There was no immunoreactivity for GYPA in vascular endothelial cell membranes (open arrows). Scale bar: 10 μm in all.
doi:10.1371/journal.pone.0033554.g005

Figure 6. Cellular and subcellular distribution of SPARC immunoreactivity in E14, E16 and adult choroid plexus. A. Embryonic day 14 (E14) lateral ventricular choroid plexus. The most lateral (older) segment of the plexus close to the tip is shown in the upper part of the figure. In this area small subsets of SPARC-immunopositive epithelial cells exhibit a fine granular immunoreactivity (open arrowheads) and a few strongly immunostained large 'vacuoles' (arrows) in contrast to neighboring epithelial cells without immunoreactivity (closed arrowheads). Note the absence of SPARC-immunostaining in perivascular spaces and in endothelial cell membranes (open arrow). **B.** E16 lateral ventricular choroid plexus. A segment of the plexus similar to that shown in **A** exhibits many strongly immunoreacting choroid plexus epithelial cells (open arrowheads). The patchy reaction product in these cells is associated with a tubulocisternal endoplasmic reticulum (TER). Note the immunostaining along the basolateral cell membranes (BM) in the strongly SPARC-immunopositive cells. A few large granules (arrows) are present in the majority of the epithelial cells including those showing low SPARC-immunoreactivity (filled arrowheads). SPARC-immunostaining is absent from perivascular spaces and endothelial cell membranes (open arrow). **C.** Adult lateral ventricular choroid plexus. Note the apparent lack of cytoplasmic immunoreactivity in the apical-most part of the epithelial cells, but the pronounced immunostaining of large 'vacuoles' (arrows) which represent a combination of multivescicular bodies and lysosomes. There was no immunoreactivity for SPARC either in perivascular spaces or in individual endothelial cell membranes. Scale bar: 10 μm in all.
doi:10.1371/journal.pone.0033554.g006

at all ages, with a peak in intensity of immunoreactivity in E15–E16 embryos (Cf. **Fig. 6A and B**). As found for GYPA, most immunoreactivity for SPARC was observed in the apical cytoplasm in the most mature choroid plexus epithelial cells of the developing choroid plexus opposite the hippocampal anlage (**Fig. 6B**). Positive immunoreactivity was visible in E13 plexus epithelial cells (not shown), and following the peak at E15–16 there was a decrease in the strength of immunostaining by P2 (not shown) and adult (**Fig. 6C**).
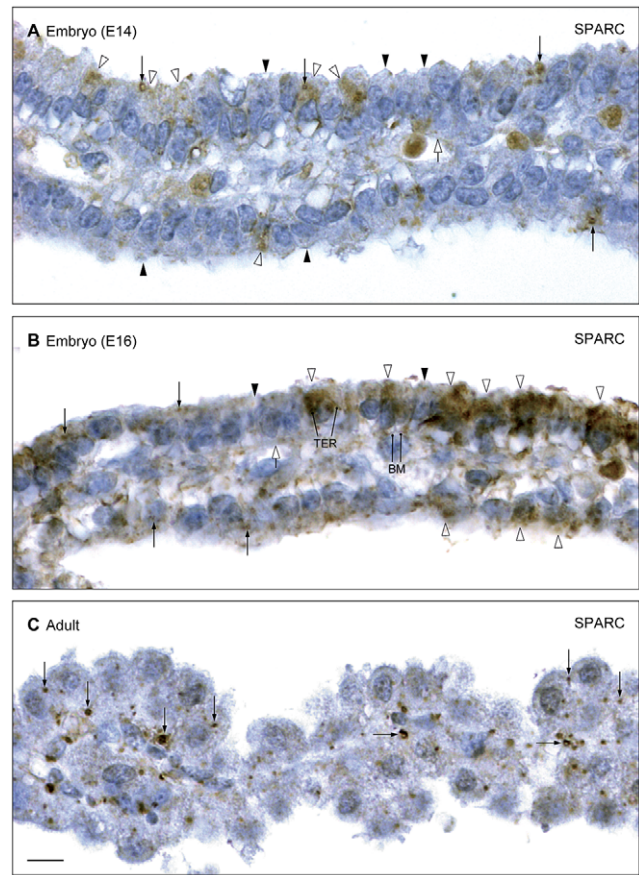
At the subcellular level a positive fine granular staining was visible in small subsets of E14 choroid plexus epithelial cells throughout the cytoplasm with spared nuclei (**Fig. 6A**). Larger dense granules were also present. The perivascular space and endothelial cells of the choroid plexus showed no reactivity for SPARC. At E16 a more pronounced SPARC immunoreactivity was present in the most apical and central part of the part of
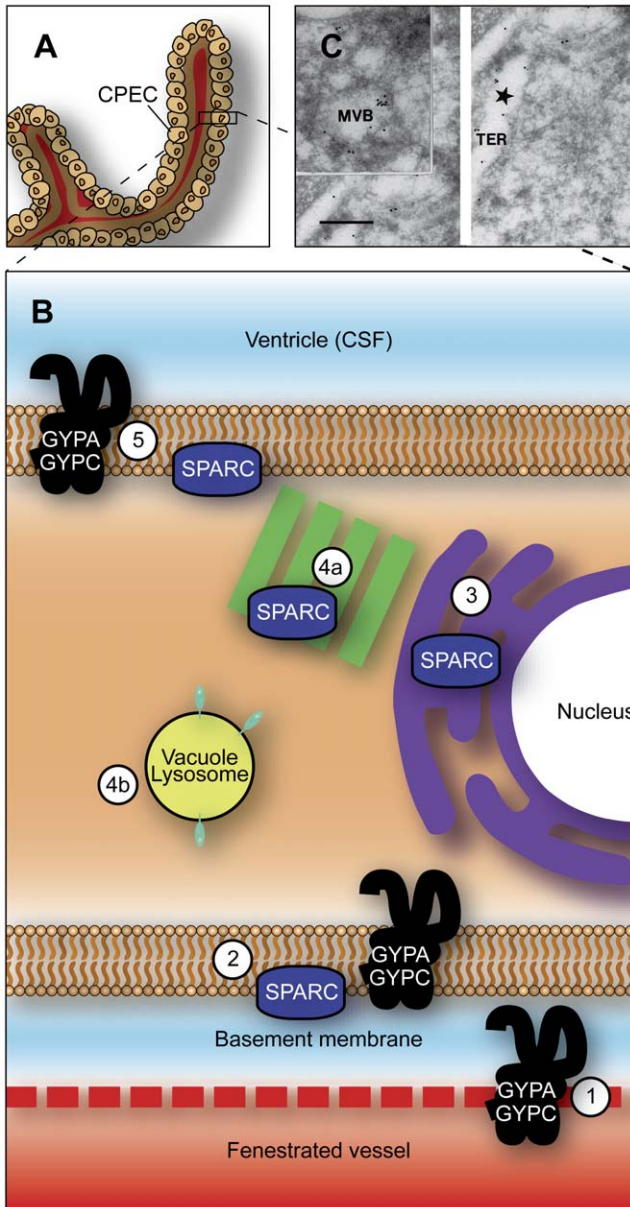
Figure 7. Proposed transepithelial pathway for albumin through choroid plexus epithelial cells. A. Whole choroid plexus showing single layer of epithelial cells sitting on thick basement membrane (see also **Fig. 1C**). **B.** Illustration depicting the suggested routes of albumin from plasma into CSF across the choroid plexus epithelium. GYPA/C in the endothelial cells may deliver albumin to the basement membrane (1) from where it can be taken up into the plexus epithelium by GYPA/C or SPARC (2). From here albumin may travel along a SPARC-specific pathway through the tubulocisternal endoplasmic reticulum (3, and see C) and Golgi (4a), or via a VAMP-mediated pathway in vacuoles, lysosomes or multivesicular bodies (4b, and see panel C). On the apical surface of the plexus epithelium, GYPA/C may be involved in efflux of protein from the cell into the CSF of the ventricles (5), as validated by extensive GYPA immunoreactivity in embryonic plexus (**Fig. 5A**). In the adult, the lack of immunoreactivity in the endoplasmic reticulum and Golgi (see **Fig. 5** and **Fig. 6**) along with increased expression of gene products for VAMP molecules (see **Fig. 3C**) suggest that the majority of transport possibly occurs via VAMP-mediated vesicular/lysosomal transport such as shown in (4b). **C.** Transmission electron micrograph of ultracryosection from E60 fetal sheep choroid plexus [87]. Immunolabelled human albumin 6 nm particles and sheep albumin 12 nm gold particles are shown to co-localise within the tubulocisternal endoplasmic reticulum. Abbrevia-

epithelial cells in the positively-reacting segments of the plexus (**Fig. 6B**). The immunostaining reaction outlined the tubulocisternal system and extended along the lateral cell membrane to the basal membrane, which was also stained (**Fig. 6B**). There was no SPARC reactivity in endothelial cells forming the stromal centre of the plexus. In the adult there was an apparent lack of fine granular cytoplasmic reactivity in the apical-most part of the epithelial cells combined with an absence of tubulocisternal-associated cytoplasmic reactivity (**Fig. 6C**). However, the basal cytoplasm of most cells showed a strong staining reaction of large 'vacuoles', multivescicular bodies and lysosomes. There was no reactivity for SPARC either in perivascular spaces or in individual endothelial cell membranes.

Vesicle-associated membrane proteins

The vesicle-associated membrane proteins (VAMP1, VAMP5 and VAMP8) are members of a family of SNARE proteins (soluble NSF attachment protein receptors), mostly involved in vesicle fusion [72–74]. There are seven members of this protein family in total: VAMP1/synaptobrevin, VAMP2, VAMP3/cellubrevin, VAMP4, VAMP5, VAMP7/Ti-vamp, and VAMP8/endobrevin [75–79]. These proteins are generally distributed in various post-Golgi structures, as well as on the plasma membrane of transporting cells. The intracellular traffic between different membrane compartments and across transporting cells involves a diverse range of membrane-enclosed intermediates, generated at plasma membranes via the action of several membrane proteins (such as the VAMP family) as well as cytosolic coat proteins [80–82].

Three *Vamp* targets were enriched in the adult lateral ventricular choroid plexus: *Vamp1* (2.3-fold), *Vamp5* (2.2-fold) and *Vamp8* (2.2-fold). The presence of the vesicle-associated membrane proteins in the epithelial cells of the lateral ventricular choroid plexus and their up-regulation in the adult supports the idea that there are two transfer mechanisms operating at the blood–CSF barrier: one specific for individual proteins; and another transfer mechanism, which is non-specific, occurring via vesicular uptake and release [18]. We confirmed GeneChip data using PCR (see **Fig. 3C**); and report enrichment of *Vamp1*, *5* and *8* in the adult mouse lateral ventricular choroid plexus. The expression of *Vamps* in plexus epithelial cells indicate that they may be involved in translocation of albumin and other plasma proteins across the choroid plexus epithelium, particularly in the adult. Thus VAMP5 is present on the outside of both the basolateral and apical membrane of the cell, helping to package molecules in both the blood and CSF and inside the cell, while VAMP1 is present on the cell membrane, working in tandem with Vamp5 [83,84]. The third family member investigated in the current study, VAMP8, is probably present in cytoplasmic endosomes of the choroid plexus epithelial cell and is involved in removing unwanted material from the cell [85,86]. Though these transcripts displayed up-regulated expression in the adult plexus, they were also present in the embryo. As mentioned above, many lysosomes were seen in the apical portion of the plexus epithelial cells that were immunopositive for the albumin-binding protein SPARC. It is possible that the SPARC-mediated recruitment of albumin into the epithelial cells of the choroid plexus on the basolateral (blood) surface is coupled with the VAMP-mediated uptake of albumin, into vesicles with exocytosis of albumin on the apical (CSF) surface into the CSF via an

endosomal/lysosomal system within the cytoplasm of the plexus epithelial cells (4b in Figure 7).

Proposed mechanism for plasma protein transport across choroid plexus epithelial cells

The present results provide additional evidence for a protein-specific transfer mechanism that contributes to regulation of the internal environment of the developing brain. Previous evidence suggested that this mechanism is particularly important in early development [16–18,20,21]. This is supported by the present finding that putative albumin receptors, SPARC, GYPA and GYPC are up-regulated in the embryonic choroid plexuses of mice, whereas expression of several members of the VAMP family of proteins is higher in the adult. These findings support the previous suggestion that two protein transfer mechanisms operate in parallel at the level of the choroid plexus epithelial cells of the blood-CSF barrier: one specific for individual plasma proteins in the blood to CSF direction, operating predominantly during early development; and a second, non-specific vesicular uptake mechanism in both blood to CSF and CSF to blood directions, operating both during early development and in the adult. The specificity of the protein specific transfer mechanism appears to be due to the presence of protein receptors on the basolateral surface of the choroid plexus epithelial cells. However, a direct link between these putative albumin transporters and albumin itself still needs to be established. These studies are in progress.

Some of the differences in subcellular distribution of SPARC and GYPA demonstrated by immunocytochemistry suggest that they may play different but complementary roles in albumin recognition and transport from blood to CSF in epithelial cells of the developing choroid plexus. A proposed mechanism for this transfer is illustrated in **Fig. 7**. Thus GYPA in the endothelial cells of vessels in the choroid plexus stroma may deliver albumin to the interstitial space from where it is taken up into the epithelial cell via the GYPA on the basolateral surface of the plexus cells. Immunoreactivity for SPARC in the tubulocisternal endoplasmic reticulum pathway (refer to **Fig. 6B**; [87,88]; see also **Fig. 7C**) early in embryogenesis suggests the involvement of SPARC in transcellular transport of albumin [86]. SPARC-immunopositivity of the Golgi apparatus confirms that this glycoprotein is synthesised by the plexus epithelial cells as also shown by the positive single cell PCR and immunocytochemistry results. In contrast, in the adult there was a lack of fine granular cytoplasmic reactivity in the apical-most part of the epithelial cells combined with an absence of tubulocisternal-associated cytoplasmic reactivity (**Fig. 6C**). However, the basal cytoplasm of most cells showed a strong staining reaction of large 'vacuoles', multivesicular bodies and lysosomes, perhaps correlating with the up-regulated VAMPs 1, 5 and 8. A summary of the steps in this proposed pathway is provided in **Fig. 7**.

Conclusions

In this study we provide a searchable resource for the elucidation of gene expression at the blood-CSF barrier in the embryonic mouse compared to the adult. This is the first gene profiling dataset available for the study of choroid plexus epithelial cells during development and we have reported a comprehensive list of transcripts enriched in the blood-CSF barrier of both the embryo and the adult. These targets encode those involved in metabolic activities, junction formation, influx and efflux transporters, protein binding and receptors.

One outcome is that it is now possible to make some comparisons between expression of specific genes in the embryonic choroid plexus and published functional data for transporters,

tight junction permeability, protein binding and receptors. The findings also help to explain number of important previous findings. For example it was reported many years ago that glutamate is toxic to the brain if administered in the neonatal period [89]. Some attributed this to "immaturity" of the blood-brain barrier [90]. However, it can now be seen that the barrier contribution to toxicity is much more likely to be due to greater transport by e.g. Slc1a4 (**Table 6**). Another example is the recent report of serotonin synthesis by the placenta that appears to be important for forebrain development [91]. Numerous serotonin receptors (HTR1-7) were found to be expressed in embryonic choroid plexus (**Table S3**) suggesting this as the site of entry of serotonin into the developing forebrain. The finding of several albumin binding proteins in the route between blood and CSF across choroid plexus epithelial cells reinforces earlier evidence for a specific protein transport mechanism in the developing choroid plexus. Thus the mechanisms responsible for the nature and control of the internal environment of the developing brain, supply of nutrients and exclusion of toxins appear to be well established in the embryonic choroid plexus

Supporting Information

Table S1 MIAME Compliance Checklist. MIAME describes the Minimum Information About a Microarray Experiment that is needed to enable the interpretation of the results of the experiment unambiguously and potentially to reproduce the results [26].
(DOCX)

Table S2 Complete data set. The spreadsheet contains a comprehensive list of probe sets from the GeneChip Mouse Exon 1.0 ST Array, with raw (normalised) data for E15 and adult mouse, fold change between embryo and adult (with a fold change cut-off of 2) and Gene Ontology classifications.
(DOCX)

Table S3 Total and plasma protein positive choroid plexus epithelial cells during normal mouse development. Data are expressed as mean ± s.e.m. rounded to the nearest whole cell. These values are for cells actually counted and represent approximately 10% of all choroid plexus epithelial cells at each age. % Total cells is the percentage of protein positive cells in relation to total plexus cell numbers. The lateral ventricular choroid plexus was not present in E12 embryos, hence no cell count data is available at this age. These data were used to select ages for microarray screening – the highest percentage of protein positive cells was seen at E15, and this age was compared with adult for the remainder of the study. *n* refers to the number of animals. *comparing youngest and oldest ages. Abbreviations: E, embryonic day; P, postnatal days.
(XLSX)

Table S4 Cell adhesion specific genes. A dataset containing probe sets from the GeneChip Mouse Exon 1.0 ST Array, with raw (normalised) data for E15 and adult mouse, fold change between embryo and adult (with a fold change cut-off of 2) and Gene Ontology classifications.
(XLSX)

Table S5 Ion channel specific genes. A dataset containing probe sets from the GeneChip Mouse Exon 1.0 ST Array, with raw (normalised) data for E15 and adult mouse, fold change between embryo and adult (with a fold change cut-off of 2) and Gene Ontology classifications.
(XLSX)

Table S6 Transporter activity specific genes. A dataset containing probe sets from the GeneChip Mouse Exon 1.0 ST Array, with raw (normalised) data for E15 and adult mouse, fold change between embryo and adult (with a fold change cut-off of 2) and Gene Ontology classifications.
(XLSX)

Table S7 Efflux transporter specific genes. A dataset containing probe sets from the GeneChip Mouse Exon 1.0 ST Array, with raw (normalised) data for E15 and adult mouse, fold change between embryo and adult (with a fold change cut-off of 2) and Gene Ontology classifications.
(XLSX)

Table S8 Protein binding specific genes. A dataset containing probe sets from the GeneChip Mouse Exon 1.0 ST Array, with raw (normalised) data for E15 and adult mouse, fold change between embryo and adult (with a fold change cut-off of 2) and Gene Ontology classifications.
(XLSX)

Author Contributions

Conceived and designed the experiments: SL ST KD NS. Performed the experiments: SL KM RG AW TP. Analyzed the data: SL ST HB H-CB KD NS. Contributed reagents/materials/analysis tools: ST H-CB NS. Wrote the paper: SL KD NS.

References

1. Saunders NR, Ek CJ, Habgood MD, Dziegielewska KM (2008) Barriers in the brain: a renaissance? Trends Neurosci 31: 279–286.
2. Daneman R, Zhou L, Agalliu D, Cahoy JD, Kaushal A, et al. (2010) The mouse blood-brain barrier transcriptome: a new resource for understanding the development and function of brain endothelial cells. PLoS One 5: e13741. doi:10.1371/journal.pone.0013741.
3. Stolp HB, Dziegielewska KM (2009) Review: Role of developmental inflammation and blood-brain barrier dysfunction in neurodevelopment and neurodegenerative diseases. Neuropathol Appl Neurobiol 35: 132–146.
4. Neuwelt EA, Bauer B, Fahlke C, Fricker G, Iadecola C, et al. (2011) Engaging neuroscience to advance translational research in brain barrier biology. Nat Rev Neurosci 12: 169–182.
5. Saunders NR, Habgood MD, Dziegielewska KM (2010) Neurotoxicology of barriers in the developing brain. In: Harry J, Tilson H, eds. Developmental Neurotoxicology. New York: Informa Health Care. pp 50–78.
6. Ek CJ, Dziegielewska KM, Habgood MD, Saunders NR (2011) Barriers in the developing brain and neurotoxicology. Neurotoxicologydoi:10.1016/j.neuro.2011.12.009.
7. Davson H, Segal MB (1996) Physiology of the CSF and blood-brain barriers. Boca Raton: CRC Press. 832 p.
8. Johansson PA, Dziegielewska KM, Liddelow SA, Saunders NR (2008) The blood-CSF barrier explained: when development is not immaturity. Bioessays 30: 237–248.
9. Saunders NR (1992) Ontogenic development of brain barrier mechanisms. In: Bradbury MWB, ed. Physiology and Pharmacology of the Blood Brain-Barrier. Handbook of Experimental Pharmacology. Berlin: Springer-Verlag. pp 327–369.
10. Ek CJ, Wong A, Liddelow SA, Johansson PA, Dziegielewska KM, et al. (2010) Efflux mechanisms at the developing brain barriers: ABC-transporters in the fetal and postnatal rat. Toxicol Lett 197: 51–59.
11. Adinolfi M, Beck SE, Haddad SA, Seller MJ (1976) Permeability of the blood-cerebrospinal fluid barrier to plasma proteins during foetal and perinatal life. Nature 259: 140–141.
12. Adinolfi M, Haddad SA (1977) Levels of plasma proteins in human and rat fetal CSF and the development of the blood-CSF barrier. Neuropadiatrie 8: 345–353.
13. Dziegielewska KM, Evans CA, Fossan G, Lorscheider FL, Malinowska DH, et al. (1980a) Proteins in cerebrospinal fluid and plasma of fetal sheep during development. J Physiol 300: 441–455.
14. Dziegielewska KM, Saunders NR (1988) The development of the blood-brain barrier in fetal and neonatal CSF, their nature, and origins. In: Meisami PJ, Timiras PJ, eds. Handbook of human growth and developmental biology. Part A: Developmental neurobiology. Boca Raton: CRC Press. pp 169–191.
15. Knott GW, Dziegielewska KM, Habgood MD, Li ZS, Saunders NR (1997) Albumin transfer across the choroid plexus of South American opossum (*Monodelphis domestica*). J Physiol 499: 179–194.
16. Dziegielewska KM, Evans CA, Malinowska DH, Møllgård K, Reynolds ML, et al. (1980b) Blood-cerebrospinal fluid transfer of plasma proteins during fetal development in the sheep. J Physiol 300: 457–465.
17. Habgood MD, Sedgwick JE, Dziegielewska KM, Saunders NR (1992) A developmentally regulated blood-cerebrospinal fluid transfer mechanism for albumin in immature rat. J Physiol 456: 181–192.
18. Liddelow SA, Dziegielewska KM, Ek CJ, Johansson PA, Potter AM, et al. (2009) Cellular transfer of macromolecules across the developing choroid plexus of *Monodelphis domestica*. Eur J Neurosci 29: 253–266.
19. Schreiber G, Aldred AR, Jaworowski A, Nilsson C, Achen MG, et al. (1990) Thyroxine transport form blood to brain via transthyretin synthesis in choroid plexus. Am J Physiol 258: R338–345.
20. Dziegielewska KM, Habgood MD, Møllgård K, Stagaard M, Saunders NR (1991) Species-specific transfer of plasma albumin into different cerebrospinal fluid compartments in the fetal sheep. J Physiol 439: 215–237.
21. Liddelow SA, Dziegielewska KM, VandeBerg JL, Noor NM, Potter AM, et al. (2011a) Modification of protein transfer across blood-CSF barrier in response to altered plasma protein composition during development. Eur J Neurosci 33: 391–400.
22. Liddelow SA, Dziegielewska KM, Møllgård K, Phoenix TN, Temple S, et al. (2011b) Sparc/osteonectin, en endogenous mechanism for targeting albumin to the blood-cerebrospinal fluid interface during brain development. Eur J Neurosci 34: 1062–1073.
23. Marques F, Sousa JC, Coppola G, Gao F, Puga R, et al. (2011) Transcriptome signature of the adult mouse choroid plexus. Fluids Barriers CNS 8: 10. doi:10.1186/2045-8118-8-10.
24. Theiler K (1989) The house mouse. Atlas of embryonic development. New York: Springer Verlag Inc. 178 p.
25. Keep RF, Jones HC (1990) A morphometric study on the development of the lateral ventricular choroid plexus, choroid plexus capillaries and ventricular ependyma in the rat. Dev Brain Res 56: 47–53.
26. Brazma A, Hingamp P, Quackenbush J, Sherlock G, Spellman P, et al. (2001) Minimum information about a microarray experiment (MIAME) – toward standards for microarray data. Nat Genet 29: 365–371.
27. Irizarry RA, Bolstad BM, Colin F, Cope LM, Hobbs B, et al. (2003) Summaries of Affymetrix GeneChip probe level data. Nucleic Acids Res 31: e15.
28. Benjamini Y, Hochberg Y (1995) Controlling the false discovery rate: a practical and powerful approach to multiple testing. J R Stat Soc Series B Stat Methodol 57: 189–300.
29. Zaykin DV, Young SS, Westfall PH (2000) Using the false discovery rate approach in the genetic dissection of complex traits: a response to Weller et al. Genetics 154: 1917–1918.
30. Zeeberg BR, Fang W, Wang G, Wang MD, Fofo AT, et al. (2003) GoMiner: a resource for biological interpretation of genomic and proteomic data. Genome Biol 4: R28.
31. Moos T, Morgan EH (2000) Transferrin and transferrin receptor function in brain barrier systems. Cell Mol Neurobiol 20: 77–95.
32. Kopp JB, Bianco P, Young MF, Termine JD, Robey PG (1992) Renal tubular epithelial cells express osteonectin in vivo and in vitro. Kidney Int 41: 56–64.
33. Stewart AK, Cheibib FT, Akbar SW, Salas MJ, Sonik RA, et al. (2011) Interactions of mouse glycophorin A with the dRTA-related mutant G719D of the mouse Cl-/HCO3- exchanger Ae1. Biochem. Cell Biol 89: 224–235.
34. Towbin H, Staehelin T, Gordon J (1979) Electrophoretic transfer of proteins from polyacrylamide gels to nitrocellulose sheets: procedure and some applications. Proc Natl Acad Sci U S A 76: 4350–4354.
35. Blazejewski S, Le Bail B, Boussarie L, Blanc JF, Malaval L, et al. (1997) Osteonectin (SPARC) expression in human liver and in cultured human liver myofibroblasts. Am J Pathol 151: 651–657.
36. Johansson PA, Dziegielewska KM, Ek CJ, Habgood MD, Liddelow SA, et al. (2006) Blood-CSF barrier function during choroid plexus development in the rat. Eur J Neurosci 24: 65–76.
37. Møllgård K, Lauritzen B, Saunders NR (1979) Double replica technique applied to choroid plexus from early foetal sheep: completeness and complexity of tight junctions. J Neurocytol 8: 139–149.
38. Bauer HC, Traweger A, Zweimueller-Mayer J, Lehner C, Tempfer H, et al. (2011) New aspects of the molecular constituents of tissue barriers. J Neural Transm 118: 7–21.
39. Ek CJ, Dziegielewska KM, Stolp HB, Saunders NR (2006) Functional effectiveness of the blood-brain barrier to small water-soluble molecules in developing and adult opossum (*Monodelphis domestica*). J Comp Neurol 496: 12–26.
40. Møllgård K, Malinowska DH, Saunders NR (1976) Lack of correlation between tight junction morphology and permeability properties in developing choroid plexus. Nature 264: 293–294.
41. Euconomopoulou M, Hammer J, Wang F, Fariss R, Maminishkis A, et al. (2009) Expression, localization, and function of junctional adhesion molecule-C (JAM-

C) in human retinal pigment epithelium. Invest Ophthalmol Vis Sci 50: 1454–1463.

42. Mertens AE, Rygiel TP, Olivo C, van der Kammen R, Collard JG (2005) The Rac activator Tiam1 controls tight junction biogenesis in keratinocytes through binding to and activation of the Par polarity complex. J Cell Biol 170: 1029–1037.

43. Kimura Y, Matsunami H, Takeichi M (1996) Expression of cadherin-11 delineates boundaries, neuromers, and nuclei in the developing mouse brain. Dev Dyn 206: 455–462.

44. Simonneau L, Thiery JP (1998) The mesenchymal cadherin-11 is expressed in restricted sites during the ontogeny of the rat brain in modes suggesting novel functions. Cell Adhes Commun 6: 431–450.

45. Aamar E, Dawid IB (2008) Protocadherin-18a has a role in cell adhesion, behaviour and migration in zebrafish development. Dev Biol 318: 335–346.

46. Steed E, Rodrigues NTL, Balda S, Matter K (2009) Identification of MarvelD3 as a tight junction-associated transmembrane protein of the occluding family. BMC Cell Biol 10: 95. doi:10.1186/1471-2121-10-95.

47. Damkier HH, Brown PD, Praetorius J (2010) Epithelial pathways in choroid plexus electrolyte transport. Physiology 25: 239–249.

48. Damkier HH, Nielsen S, Praetorius J (2007) Molecular expression of SLC4-derived Na+-dependent anion transporters in selected human tissues. Am J Physiol Regul Integr Comp Physiol 293: R2136–2146.

49. Bradbury MW, Crowder J, Desai S, Reynolds JM, Saunders NR (1972) Electrolytes and water in the brain and cerebrospinal fluid of the foetal sheep and guinea-pig. J Physiol 227: 591–610.

50. Amtorp O, Sørensen SC (1974) The ontogenetic development of concentration differences for protein and ions between plasma and cerebrospinal fluid in rabbits and rats. J Physiol 243: 387–400.

51. Johansson PA, Dziegielewska KM, Ek CJ, Habgood MD, Møllgård K, et al. (2005) Aquaporin-1 in the choroid plexus of developing mammalian brain. Cell Tissue Res 322: 353–364.

52. Grijota-Martinez C, Samarut E, Scanlan TS, Morte B, Bernal J (2011) In vivo activity of the thyroid hormone receptor beta- and α-selective agonists GC-24 and CO23 on rat liver, heart, and brain. Endocrinology 152: 1336–1342.

53. Kinne A, Schülein R, Krause G (2011) Primary and secondary thyroid hormone transporters. Thyroid Res 4: S7.

54. Chen B, Jiang Y, Zeng S, Yan J, Li X, et al. (2010) Endocytic sorting and recycling require membrane phosphatidylserine asymmetry maintained by TAT-1/CHAT-1. PLoS Genet 6: e1011235.

55. Baños G, Daniel PM, Pratt OE (1978) The effect of age upon the entry of some amino acids into the brain, and their incorporation into cerebral protein. Dev Med Child Neurol 20: 335–246.

56. Braun LD, Cornford EM, Oldendorf WH (1980) Newborn rabbit blood-brain barrier is selectively permeable and differs substantially from the adult. J Neurochem 34: 147–152.

57. Cornford EM, Braun LD, Oldendorf WH (1982) Developmental modulations of blood-brain barrier permeability as an indicator of changing nutritional requirements in the brain. Pediatr Res 16: 324–328.

58. Lefauconnier J-M, Trouvé R (1983) Developmental changes in the pattern of amino acid transport at the blood-brain barrier in rats. Dev Brain Res 6: 175–182.

59. Choudhuri S, Cherrington NJ, Li N, Klaassen CD (2003) Constitutive expression of various xenobiotic and endobiotic transporter mRNAs in the choroid plexus of rats. Drug Metab Dispos 31: 1337–1345.

60. Jauniaux E, Watson A, Ozturk O, Quick D, Burton G (1999) In-vivo measurement of intrauterine gases and acid-base values early in human pregnancy. Hum Reprod 14: 2901–2904.

61. Krishnaumurthy P, Ross DD, Nakanishi T, Bailey-Dell K, Zhou S, et al. (2004) The stem cell marker BCRP/ABCG2 enhances hypoxic cell survival through interactions with heme. J Biol Chem 279: 24218–24225.

62. Stewart PA (2000) Endothelial vesicles in the blood-brain barrier: are they related to permeability? Cell Mol Neurobiol 20: 149–163.

63. Furthmayr H, Metaxas MN, Metaxas-Buhler M (1981) Mg and Mc: mutations within the amino-terminal region of glycophorin A. Proc Natl Acad Sci U S A 78: 631–635.

64. Krotkiewski H, Lisowska E, Angel AS, Nilsson B (1988) Structural analysis by fast atom-bombardment mass spectrometry of the mixture of alditols derived from the O-linked oligosaccharides of murine glycophorins. Carbohydr Res 184: 27–38.

65. Rogalski TM, Williams BD, Mullen GP, Moerman DG (1993) Products of the unc-52 gene in Caenorhabditis elegans are homologous to the core protein of the mammalian basement membrane heparin sulfate proteoglycan. Genes Dev 7: 1471–1484.

66. Kramer JM (2005) Basement membranes. In: The C. elegans Research Community, editors (2005) WormBook, doi/10.1895/wormbook.1.16.1, Available: http://www.wormbook.org.

67. Swaroop A, Hogan BL, Francke U (1988) Molecular analysis of the cDNA for human SPARC/osteonectin/BM-40: sequence, expression, and localization of the gene to chromosome 5q31-q33. Genomics 2: 37–47.

68. Colombo MP, Ferrari G, Biondi G, Galasso D, Howe CC, et al. (1991) Downregulation of SPARC/osteonectin/BM-40 expression in methylcholan-threne-induced fibrosarcomas and in Kirsten-MSV transformed fibroblasts. Eur J Cancer 27: 58–62.

69. Maurer P, Sasaki T, Mann K, Gohring W, Schwarzbauer JE, et al. (1997) Structural and functional characterization of the extracellular calcium-binding protein BM-40/secreted protein, acidic, rich in cysteine/osteonectin from the nematode Caenorhabditis elegans. Eur J Biochem 248: 206–216.

70. Motamed K (1999) SPARC (osteonectin/BM-40). Int J Biochem Cell Biol 31: 1363–1366.

71. Schwarzbauer JE, Spencer CS (1993) The Caenorhabditis elegans homologue of the extracellular calcium binding protein SPARC/osteonectin affects nematode body morphology and mobility. Mol Biol Cell 4: 941–952.

72. Steegmaier M, Klumperman J, Foletti DL, Yoo JS, Scheller RH (1999) Vesicle associated membrane protein 4 is implicated in trans-Golgi network trafficking. Mol Biol Cell 10: 1957–1972.

73. Yang B, Gonzalez L, Jr., Prekeris R, Steegmaier M, Advani RJ, et al. (1999) SNARE interactions are not selective. Implications for membrane fusion specificity, J Biol Chem 274: 5649–5653.

74. Chung I, Burkart A, Szmydynger-Chodobska J, Dodd KA, Trimble WS, et al. (2003) Expression of two membrane fusion proteins, synaptosome associated protein of 25 kDa and vesicle-associated membrane protein, in choroid plexus epithelium. Neuroscience 116: 349–357.

75. Rothman JE, Wieland FT (1996) Protein sorting by transport vesicles. Science 272: 227–234.

76. Hong W (1998) Protein transport from the endoplasmic reticulum to the Golgi apparatus. J Cell Sci 111: 2931–2839.

77. Antonny B, Schekman R (2001) ER export: public transportation by the COPII coach. Curr Opin Cell Biol 13: 438–443.

78. Boehm M, Bonifacino JS (2001) Adaptins: the final recount. Mol Biol Cell 12(10): 2907–2920.

79. Stephens DJ, Pepperkok R (2001) Illuminating the secretory pathway: when do we need vesicles? J Cell Sci 114: 1053–1059.

80. Zerial M, McBride H (2001) Rab proteins as membrane organizers. Nat Rev Mol Cell Biol 2: 107–117.

81. Whyte JR, Munro S (2002) Vesicle tethering complexes in membrane traffic. J Cell Sci 115: 2627–2637.

82. Zeng Q, Tran TT, Tan HX, Hong W (2003) The cytoplasmic domain of Vamp4 and Vamp5 is responsible for their correct subcellular targeting: the N-terminal extension of Vamp4 contains a dominant autonomous targeting signal for the trans-Golgi network. J Biol Chem 278: 23046–23054.

83. Jahn R, Südhof TC (1999) Membrane fusion and exocytosis. Annu Rev Biochem 68: 863–911.

84. Khvotchev MV, Südhof TC (2004) Stimulus-dependent dynamic homo- and heteromultimerization of synaptobrevin/VAMP and synaptophysin. Biochemistry 43: 15037–15043.

85. Palade G (1975) Intracellular aspects of the process of protein synthesis. Science 189: 347–358.

86. Wong SH, Zhang T, Xu Y, Subramaniam VN, Griffiths G, et al. (1998) Endobrevin, a novel synaptobrevin/VAMP-like protein preferentially associated with the early endosome. Mol Biol Cell 9: 1549–1563.

87. Møllgård K, Saunders NR (1977) A possible transepithelial pathway via endoplasmic reticulum in foetal sheep choroid plexus. Proc R Soc Lond B Biol Sci 199: 321–326.

88. Balslev Y, Dziegielewska KM, Møllgård K, Saunders NR (1997) Intercellular barriers to and transcellular transfer of albumin in the fetal sheep brain. Anat Embryol 195: 229–236.

89. Olney JW, Ho OL (1970) Brain damage in infant mice following oral intake of glutamate, aspartate or cysteine. Nature 227: 609–611.

90. Viña JR, DeJoseph MR, Hawkins PA, Hawkins RA (1997) Penetration of glutamate into brain of 7-day-old rats. Metab Brain Dis 12: 219–227.

91. Bonnin A, Goeden N, Chen K, Wilson ML, King J, et al. (2011) A transient placental source of serotonin for the fetal forebrain. Nature 472: 347–350.

92. Porterfield SP, Hendrich CE (1992) Tissue iodothyronine levels in fetuses of control and hypothyroid rats at 13 and 16 days gestation. Endocrinology 131: 195–200.

93. Morgan EH, Moos T (2002) Mechanism and developmental changes in iron transport across the blood-brain barrier. Dev Neurosci 24: 106–113.

94. Al-Sarraf H (2002) Transport of 14C-gamma-aminobutyric acid into brain, cerebrospinal fluid and choroid plexus in neonatal and adult rats. Brain Res Dev Brain Res 139: 121–129.

95. Al-Sarraf H, Preston JE, Segal MB (1997) Changes in the kinetics of the acidic amino acid brain and CSF uptake during development in the rat. Dev Brain Res 102: 127–134.

96. Chowanadisai W, Kelleher SL, Lönnerdal B (2005) Zinc deficiency is associated with increased brain zinc import and LIV-1 expression and decrease ZnT-1 expression in neonatal rats. J Nutr 135: 1002–1007.